Available online at www.sciencedirect.com
ScienceDirect
Journal of Theoretical Biology 244 (2007) 15–45
Journal of Theoretical Biology
www.elsevier.com/locate/yjtbi

Mathematical analysis of trabecular 'trajectories' in apparent trajectorial structures: The unfortunate historical emphasis on the human proximal femur

John G. Skedros[a,b,*], Sidney L. Baucom[b]

[a]*University of Utah Department of Orthopaedic Surgery, and the Bone and Joint Research Laboratory, Department of Veterans Affairs Medical Center, Salt Lake City, UT, USA*
[b]*Utah Bone and Joint Center, 5323 South Woodrow Street, Suite 202, Salt Lake City, UT 84107, USA*

Received 29 November 2005; received in revised form 22 June 2006; accepted 22 June 2006
Available online 5 July 2006

Abstract

Wolff's "law" of the functional adaptation of bone is rooted in the trajectory hypothesis of cancellous bone architecture. Wolff often used the human proximal femur as an example of a trajectorial structure (i.e. arched trabecular patterns appear to be aligned along tension/compression stress trajectories). We examined two tenets of the trajectory hypothesis; namely, that the trabecular tracts from the tension- and compression-loaded sides of a bending environment will: (1) follow 'lines' (trajectories) of tension/compression stress that resemble an arch with its apex on a neutral axis, and (2) form orthogonal (90°) intersections. These predictions were analysed in proximal femora of chimpanzees and modern humans, and in calcanei of sheep and deer. Compared to complex loading of the human femoral neck, the chimpanzee femoral neck reputedly receives relatively simpler loading (i.e. temporally/spatially more consistent bending), and the artiodactyl calcaneus is even more simply loaded in bending. In order to directly consider Wolff's observations, measurements were also made on two-dimensional, cantilevered beams and curved beams, each with intersecting compression/tension stress trajectories. Results in the calcanei showed: (1) the same nonlinear equation best described the dorsal ("compression") and plantar ("tension") trabecular tracts, (2) these tracts could be exactly superimposed on the corresponding compression/tension stress trajectories of the cantilevered beams, and (3) trabecular tracts typically formed orthogonal intersections. In contrast, trabecular tracts in human and chimpanzee femoral necks were non-orthogonal (mean ~70°), with shapes differing from trabecular tracts in calcanei and stress trajectories in the beams. Although often being described by the same equations, the trajectories in the curved beams had lower r^2 values than calcaneal tracts. These results suggest that the trabecular patterns in the calcanei and stress trajectories in short beams are consistent with basic tenets of the trajectory hypothesis while those in human and chimpanzee femoral necks are not. Compared to calcanei, the more complexly loaded human and chimpanzee femoral necks probably receive more prevalent/predominant shear, which is best accommodated by non-orthogonal, asymmetric trabecular tracts. The asymmetrical trabecular patterns in the proximal femora may also reflect the different developmental 'fields' (trochanteric vs. neck/head) that formed these regions, of which there is no parallel in the calcanei.
Published by Elsevier Ltd.

Keywords: Wolff's law; Trajectory hypothesis; Stress trajectories; Cancellous bone adaptation; Cancellous bone anisotropy; Trabecular bone

1. Introduction and historical background

> "By wondering about what mathematical rules bone architecture might be the answer to, we do not learn anything useful at all. The key to information is in the metabolic process of bone production and maintenance." (Huiskes, 2000, p. 154)

Anisotropic patterns in the trabecular architecture of cancellous bone are commonly used to infer local loading history in extant and extinct animals (Black, 2004; Cheal et al., 1987; Fajardo and Muller, 2001; Herrera et al., 2001; Macchiarelli et al., 1999; Martinón-Torres, 2003; Oxnard

*Corresponding author. Utah Bone and Joint Center, 5323 South Woodrow Street, Suite 202, Salt Lake City, Utah 84107, USA.
Tel.: +1 801 713 0606; fax: +1 801 713 0609.
E-mail address: jskedros@utahboneandjoint.com (J.G. Skedros).

0022-5193/$ - see front matter Published by Elsevier Ltd.
doi:10.1016/j.jtbi.2006.06.029

and Yang, 1981; Pontzer et al., 2006; Richmond et al., 2004; Rook et al., 1999; Ryan and Ketcham, 2005a; Sabry et al., 2000; Schatzker, 1984; Swartz et al., 1998; Teng and Herring, 1995; Tillman et al., 1985; Tobin, 1968; Ward and Sussman, 1979; Zylstra, 2000). For example, arched trabecular patterns are often interpreted as adaptations that approximate the 'trajectories' of principal tension and compression stresses produced by habitual (stereotypical) bending (Bacon et al., 1984; Biewener et al., 1996; Black, 2004; Fox, 2003; Francillon-Vieillot et al., 1990; Hayes and Snyder, 1981; Lanyon, 1974; Pauwels, 1976; Thomason, 1995; Vander Sloten and Van der Perre, 1989; Venieratos et al., 1987; Viola, 2002). This interpretation largely originates with Julius Wolff's formulation of the trajectory 'theory' of cancellous bone architecture (Wolff, 1869, 1870, 1872, 1874, 1892, 1986; Zippel, 1992). Murray (Murray, 1936, pp. 99–100) summarized this succinctly as: "The fundamental idea in the trajectorial theory of bone structure is that the trabeculae of cancellous bone follow the lines of trajectories in the homogenous body of the same form as the bone and stressed in the same way." An additional integral tenet of the trajectory 'theory' (more correctly a hypothesis, see Appendix) is that the opposing stress trajectories (i.e. principal tension and compression trajectories) form orthogonal (90°) intersections.

The trajectory hypothesis played a central role in the intellectual development of 'Wolff's "law" of the transformation of bone'. In a general context, Wolff's "law" can be stated as: "Every change in the form and function of the bones, or of their function alone, is followed by certain definite changes [or "transformations"] in their internal architecture, and equally definite secondary alterations of their external conformation, in accordance with mathematical laws" (Freiberg, 1902). Similar translations referring to "mathematical laws" or "rules" have been used by numerous authors (e.g. Bertram and Swartz, 1991; Brand et al., 2003; Field and Kenyon, 1989; Frost, 1988b; Keith, 1919; Löer and Weigmann, 1992; Morris, 1971; Rasch and Burke, 1978; Rubin, 1988; Rubin and Hausman, 1988; Treharne, 1981; Zippel, 1992). Wolff's "law" is based on Wolff's observations suggesting relationships (causal in some cases) between static mechanical forces and cortical/cancellous bone "transformations" in various situations including normal development and fracture healing (Bertram and Swartz, 1991; Dibbets, 1992; Huiskes et al., 1981; Roesler, 1981; Wolff, 1892). While formulation of this "law" explains trabecular orientation of cancellous bone as being aligned along the principal lines of stress, it has also been adopted to explain the mechanical adaptation of bones and other connective tissues in more general contexts (Akeson et al., 1992; Arem and Madden, 1974; Bertram and Swartz, 1991; Biewener et al., 1986; Brickley-Parsons and Glimcher, 1984; Burger et al., 2003; Forrester et al., 1970; Holt et al., 2004; Joshi et al., 2000; Kennedy, 1989; Kumaresan et al., 2001; Reddy et al., 2002; Stanford and Schneider, 2004; Treharne, 1981; Whedon and Heaney, 1993; Woo et al., 1981). The influence of Wolff's seminal work is pervasive, as evidenced by nearly 690 recorded citations from 1980 to 2005 of his treatise of 1892 and the published translation of 1986 (Science Citation Index—Citrix, ISI databases, Institute for Scientific Information, Philadelphia, PA).

Among a variety of bones exhibiting arched trabecular patterns, the human proximal femur was Wolff's cardinal example of a natural trajectorial structure (Wolff, 1892, 1986; Zippel, 1992). The interpretation that the trabecular arches in this bone follow the 'lines' of tension and compression stresses is still common in contemporary literature (Bagi et al., 1997; Barbieri and Buoncristiani, 1975; Baumgaertner and Higgins, 2002; Beck et al., 1990; Berquist and Coventry, 1992; Brown and DiGioia, 1984; Bullough and Vigorita, 1984; Chapman and Zickel, 1988; Cowin, 1984; Elke et al., 1995; Fazzalari et al., 1989; Finlay et al., 1991; Fox, 2003; Ganey and Ogden, 1998; Gibson and Ashby, 1997; Greenspan, 1988; Herrera et al., 2001; Kapandji, 1987; Kawashima and Uhthoff, 1991; Kerr et al., 1986; Kerr and Bishop, 1986; Knothe Tate, 2003; Koval and Zuckerman, 2002; Kyle, 1994; Laroche et al., 1995; Laros, 1990; Lim et al., 1999; Lotz et al., 1995; Maquet, 1985; Markolf, 1991; Martini, 1995; Miller, 1996; Miller et al., 2002; Moore, 1985; Mourtada et al., 1996; Neville, 1993; Oatis, 2004; Osborne et al., 1980; Radin et al., 1992; Resnick and Niwayama, 1988; Rosenthal and Scott, 1983; Schatzker, 1984, 1991; Sinclair and Dangerfield, 1998; Tachdjian, 1990; Van Audekercke and Van der Perre, 1994; Vander Sloten and Van der Perre, 1989; Venieratos et al., 1987). However, recent authors who have reviewed the historical and/or current use of the trajectorial hypothesis in this context suggest that principal tension and compression stresses or strains do not play a proximate causal role in the formation of these distinctive trabecular patterns (discussed later) (Carter and Beaupré, 2001; Cowin, 2001; Hall, 1985; Huiskes, 2000; Huiskes et al., 1981; Kriz et al., 2002; Roesler, 1981).

The seeds of the trajectorial hypothesis were planted in 1866 when the notable engineer and mathematician Karl Culmann suggested to the anatomist G.H. von Meyer that arched trabecular patterns in a sagittally sectioned human first metatarsal and calcaneus appear to be aligned along principal stress directions engendered by functional loading (Rüttimann, 1992; Thompson, 1917, 1943; von Meyer, 1867). Evidently, Culmann drew an analogy between these trabecular patterns and the stress trajectories of a short, cantilevered beam illustrated in his textbook "Die Graphishe Statik" ("Graphical Statics") (Culmann, 1866) (Figs. 1 and 2). Culmann and von Meyer also compared the trabecular architecture in a coronally (frontally) sectioned human proximal femur to the mathematically constructed stress trajectories of a curved crane-like beam that resembled a human femur (without trochanters) loaded in single-legged stance (see Appendix A for further discussion of the origins of Culmann's 'crane'). Notably, the arched trabecular patterns in the von Meyer femur do not form orthogonal intersections as they clearly do in the

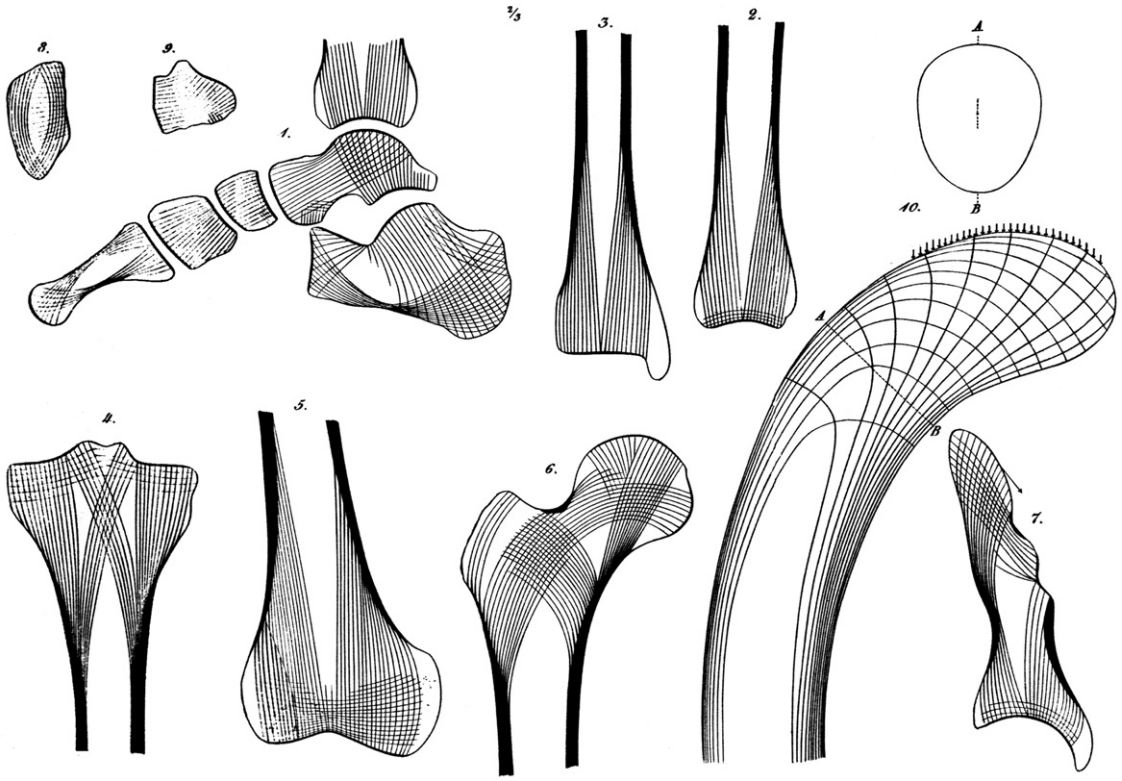

Fig. 1. von Meyer's (1867) composite illustration shows the Culmann 'crane' and sections of various human bones with stylized arching trabecular patterns. According to Rüttimann (1992, p. 14), the original figure legend reads: This graphic gives a modification of the curved crane that Prof. Culmann had designed [see Fig. 3 of the current study] under his control with the intention of approximately imitating the shape of the upper end of the femur and the transverse section of the neck and presuming the same wide strain as the head of the femur receives from the socket. (Reproduced from the original with permission of Walter de Gruyter, Berlin, Germany. 1992. Text chapter by Rüttimann In Wolff's Law and Connective Tissue Regulation. p. 15. Fig. 1).

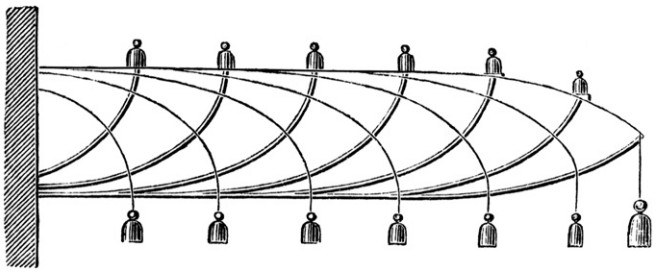

Fig. 2. Culmann's (1866, Fig. 107, p. 236) short, cantilevered beam with stress trajectories. This beam is reproduced in several of Wolff's works (e.g. 1870, 1892, 1986). (Reproduced with the permission of Springer-Verlag, Berlin).

Culmann 'crane' (compare these drawings in Fig. 1). To our knowledge, however, von Meyer, did not mathematically analyse the course of apparent "tension" and "compression" curvilinear trabecular patterns, and did not further rigorously consider the implications of the non-orthogonal intersections that he illustrated in this drawing of a human proximal femur (Löer and Weigmann, 1992; Zippel, 1992).

Recognizing this discrepancy—with what he perceived to be *orthogonal* trabecular patterns in his own proximal femoral sections—Wolff admonished von Meyer for not drawing the femoral trabecular patterns "correctly" (Wolff, 1869; this paper was not illustrated). In contrast to von Meyer's femur drawing (Fig. 1), Wolff's composite illustration of 1870 shows orthogonally intersecting trabecular arches in a diagrammatic drawing of a coronally sectioned human proximal femur (Fig. 3).[1] Wolff, convinced that the similarities between trajectories in Culmann's 'crane' and the arched trabecular patterns in the human proximal femur could not be coincidental, hypothesized that "…the direction and pattern of loading influences, and/or controls, the pattern of the trabecular framework"—hence the origin of Wolff's emphasis on "mathematical laws" (i.e. that there is a direct mathematical relationship between bone form and skeletal loads) (Bertram and Swartz, 1991; Zippel, 1992).[2] Wolff (1892)

[1]The provenance of Wolff's (1870) early illustration of the femur as trajectorial structure has been confused in recent literature. For example, Wolff's trajectorial femur (see drawing of it in Fig. 3) has been erroneously attributed to G.H. von Meyer (e.g., see (Cowin, 1986, 1989b, 2001; Huiskes, 2000; Miller et al., 2002). Thompson (1917, p. 682) also made the same error, but he later corrected it (Thompson, 1943, p. 978). Other authors have re-drawn the Culmann 'crane' with non-orthogonal trajectories apparently to resemble those of von Meyer's femur (Thomason, 1995).

[2]See the Appendix A for the "proofs" that Wolff offered in support for the trajectory hypothesis in explaining the functional/causal relationships of the arched trabecular patterns in the cancellous bone architecture of the femoral neck.

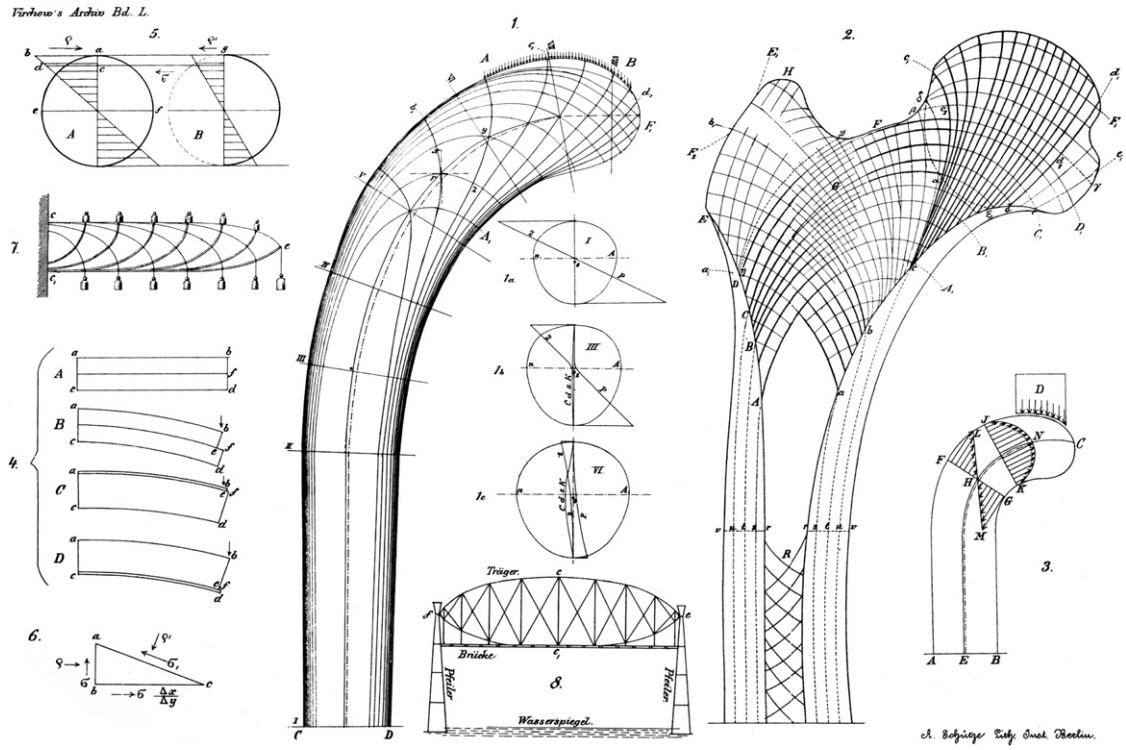

Fig. 3. Wolff's (1870) composite diagram (which includes reproductions of Culmann's cantilevered beam and 'crane') (see Figs. 1 and 2). Wolff obtained the drawing of the 'crane' and most of the other structures from Culmann (Wolff, 1870, 1892) (see further discussion in the Appendix A) (Reproduced from the original with the permission of ASME, New York, NY). The original figure legend reads (translated by Jos Dibbets, with his comments (J.D.) indicated in brackets): Plate XII Fig. 1. Illustration of forces and trajectories that act on the interior of a bone. After the original, drawn by students of Prof. Culmann and under his supervision, notably to twice the size of a human femur. This original drawing was first photographically reduced to natural dimensions and then lithographed. Fig. 1a–c, depict the force layout for the selected cross-section examples I, III, and VI. [*Note*: Culmann's technique assumed a solid interior, not a tube-like construction. JD], Fig. 2. Schematic reproduction of the photographed specimen from Fig. 1 Plate X. Figs. 3–7 relate to the explanation of the "graphical static" [method] on pp. 402–407. [Note on "graphischen Statik": Culmann apparently developed a method to draw force trajectories instead of making elaborate calculations on strength. JD], Fig. 8. Schematic illustration of a bridge built according to the Pauly system.

also suggested that in some cases predominant patterns of trabecular orientation could be 'transformed' by alterations in loading patterns (e.g. in a malunited femoral neck fracture, or in an ankylosed knee), and that, in equilibrium, preferred trabecular patterns represent the 'average' loading regime experienced by a bone region (Bertram and Swartz, 1991; Pauwels, 1976). Wolff's contemporaries, typically publishing in German, contested the trajectory hypothesis primarily on their observations of non-orthogonal intersections of cancellous bone trabeculae in various bones (Albert, 1900a; Bähr, 1899; Büdinger, 1903; Solger, 1899; Zschokke, 1892). Despite these contemporary objections and abundant subsequent descriptions of bones exhibiting non-orthogonality (Albert, 1900b; Carey, 1929; Jansen, 1920; Murray, 1936; Triepel, 1922), the apparent mathematical validation by the American anatomist J.C. Koch (1917) seems to have established the palatability of this idea in the English-language literature, which persists in many contemporary investigations and textbooks (Chapman and Zickel, 1988; Elke et al., 1995; Ganey and Ogden, 1998; Kapandji, 1987; Koval and Zuckerman, 2002; Lanyon, 1974; Lanyon and Rubin, 1985; Miller, 1996; Sinclair and Dangerfield, 1998). However, the mechanisms that mediate such trabecular anisotropy are still debated (Carter and Beaupré, 2001; Cowin, 2001; Huiskes, 2000), and currently with renewed interest in comparative anatomical contexts (Biewener et al., 1996; Cheal et al., 1987; Kriz et al., 2002; Pontzer et al., 2006; Skedros et al., 2002; Skedros and Brady, 2001).

Lanyon (1973, 1974) used in vivo strain measurements on sheep calcanei to show the first "clear example" of the close correspondence between arched trabecular patterns and orientations of principal strains (Bouvier, 1985; Currey, 1984) (Fig. 4). He described this bone as a cantilevered beam-like structure that typically experiences a relatively simple loading regime exhibiting two quasi-parabolic-shaped trabecular tracts that intersect to form the shape of an arch. Recording strains from rosette gauges attached directly to the bone, Lanyon determined that during ambulation the "…principal compressive strain coincided with the trabeculae in the dorsal tract and the principal tensile strain with those in the plantar tract" (Lanyon, 1974, p. 166). These data have been corroborated in a recent ex vivo study using simulated loading of deer calcanei with up to seven rosette strain gauges on each bone (Su, 1998; Su et al., 1999). Additionally, in these

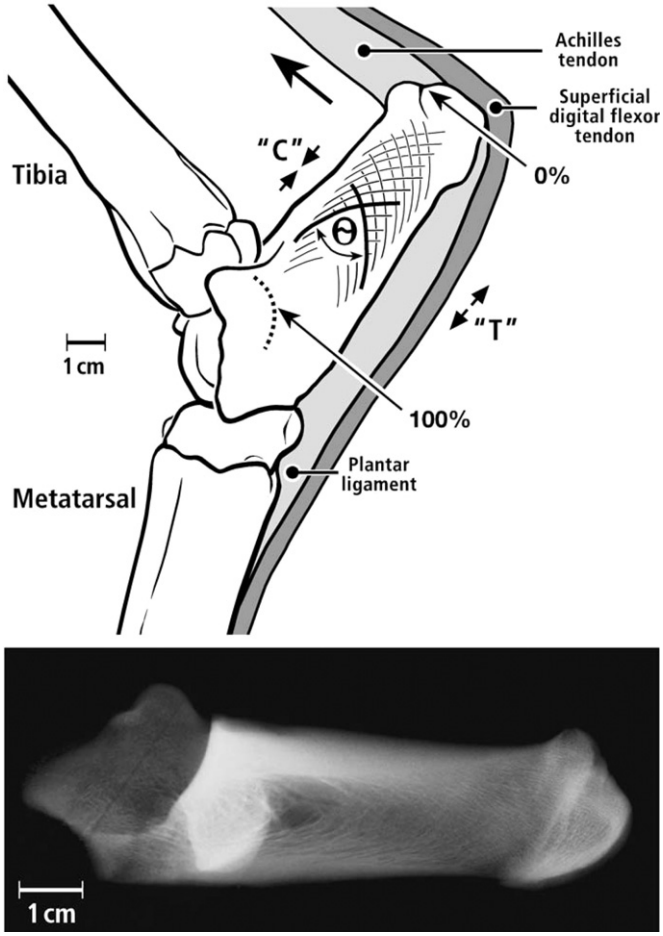

Fig. 4. At top is a lateral-to-medial view of the left ankle region of a skeletally mature mule deer showing the calcaneus, shaft length, and other associated bones, ligaments, and tendons. The trabecular patterns are stylized and are based on a medial-to-lateral roentgenogram. The dotted line at the tip of the 100% arrow indicates the projected location of the contour formed by the talus-calcaneus articular surfaces. The large dorsal-directed arrow indicates the direction of force imparted by the Achilles tendon during mid-stance, loading the dorsal cortex in compression ("C") and plantar cortex in tension ("T") (Su et al., 1999). θ indicates the location where angle measurements were made in the sheep and deer calcanei. At bottom is a lateral roentgenogram of an isolated right calcaneus from a mature animal.

studies off-axis loading designed to simulate extremes of twisting, turning, and jumping showed that the dorsal/plantar compression/tension strain distribution was highly consistent (Su, 1998). Recent in vivo strain data on calcanei of potoroos (small kangaroo-like marsupials) are also consistent with these studies and Lanyon's findings (Biewener et al., 1996). Although, to our knowledge in vivo strains have never been reliably measured on opposing cortices of metaphyseal–epiphyseal regions (e.g. femoral neck) of normal (e.g. without prosthetic devices) human femora,[3] Lanyon explicitly suggested that these findings in the sheep calcaneus are applicable to the controversial conventional interpretation of the human proximal femur as a 'tension/compression' region (Lanyon, 1974; Skedros and Bloebaum, 1991). Lanyon, however, did not quantitatively compare trabecular structural anisotropy or other morphologic features in these two bones.

Although a limitation of all of these studies of relatively simply loaded bones is that strains measured on cortical bone might not closely reflect the magnitudes and/or distributions of the strains produced in the deeper trabecular bone (Bay et al., 1999; Keaveny, 2001; Van Rietbergen et al., 2003), in vitro strain measurements made on cortical surfaces coupled with computational studies of functional loading of the human proximal femur have typically lead to the conclusion that this region can be considered as a cantilevered beam, which has become the "gold standard" for many biomechanical analyses of the femoral neck (e.g. Beck et al., 1990; Carter et al., 1989; Cristofolini et al., 1996; Demes et al., 2000; Frankel, 1960; Huiskes et al., 1981; e.g. Kummer, 1959; Martin et al., 1998; Phillips et al., 1975) (For a contrasting opinion, see Mourtada et al. (1996) who used a curved beam model, which also showed tension/compression stresses prevailing across the superior/inferior neck in single-legged stance). Although many investigators have examined Wolff's trajectory hypothesis in the context of functional loading of the human proximal femur (Carey, 1929; Carter and Beaupré, 2001; Cowin, 2001; Garden, 1961; Harty, 1984; Möser and Hein, 1987; Pauwels, 1976; Tobin, 1955, 1968), there is evidence suggesting that this region may not be an appropriate paradigm for testing this hypothesis. For example, in a two-dimensional finite element analysis, Carter et al. (1989) argue that not only are trabecular intersections in the human proximal femur non-orthogonal, but trabecular orientations do not correspond with the principal stress directions of any one loading condition. Other investigators suggest that the similarity between trabecular orientation and stress trajectories from a habitual bending moment may be circumstantial, not causal (Carey, 1929; Farkas et al., 1948; Heřt, 1992, 1994; Huiskes, 2000). In a two-dimensional finite element analysis, Pidaparti and Turner (1997) suggest that,

[3]Several investigators have telemetrically measured in vivo forces imparted to hip endoprostheses during typical ambulatory activities (Bergmann et al., 2001; Davy et al., 1988; Hodge et al., 1986; Rydell, 1966). But using indirect measurements to infer habitual strain distributions are confounded by several variables including the perturbation of the normal loading environment caused by intramedullary loading and altered muscle mechanics. Biewener et al. (1983) provide a poignant example of how indirect or incomplete analyses of a bone's strain environment can lead to erroneous conclusions about its predominant loading environment. Aamodt et al. (1997) have reported the only in vivo strain measurements on the human proximal femur that we are aware of. In this study one rosette strain gauge was placed laterally on the inferior aspect of the greater trochanter in two adult patients. The data showed that in nearly all loading regimes (e.g. two-legged stance, one-legged stance, walking, and stair climbing) the absolute magnitudes of tensile strain significantly exceeded compressive strain. Such measurements suggest that this region of the femur is subjected to bending and that "…no functional lateral tension band or medially directed force is sufficient to outweigh the bending moment imposed by the joint force" (Aamodt et al., 1997, p. 931).

compared to orthogonal trabecular intersections, *non*-orthogonal intersections may represent a more optimal design for accommodating *shear* stresses that are presumably prevalent in the human femoral neck. In contrast to the human proximal femur, the principal trabecular tracts with orthogonal intersections have been described in calcanei of deer, sheep, and potoroos (Biewener et al., 1996; Skedros and Brady, 2001). In view of these data, it has been suggested that there may be significant differences in the biophysical stimuli and the developmental 'fields' that mediate the construction of the curvilinear trabecular patterns in these disparate bone types (Kriz, 2002; Kriz et al., 2002). If mechanical stimuli are significant in the development of the cancellous architecture of these bones, then the differences in trabecular patterns may be related to the notable differences in the relative complexity of their habitual loading: complex multi-directional/multi-axial loading of the human proximal femur vs. relatively simple uni-axial bending of the artiodactyl calcaneus (Kalmey and Lovejoy, 2002; Ryan and Ketcham, 2005a; Skedros et al., 2002). The present study evaluates the trajectorial hypothesis in the context of this dichotomy.

Since the origin of Wolff's trajectory hypothesis can be traced to Culmann's short, cantilevered beam (Fig. 2) (Roesler, 1981), we examined adult artiodactyl (sheep and deer) calcanei, which generally appear to be a natural paradigm in this context. Trabecular patterns in adult chimpanzee and human proximal femora were also examined because of their putative disparate loading conditions (*human*: predominantly compression and torsion; *chimpanzee*: predominantly bending) (Kalmey and Lovejoy, 2002; Skedros et al., 1999). Analysis of trabecular architecture in these disparate loading conditions may help to clarify the applicability of Wolff's trajectory hypothesis in skeletal biology and advance our understanding of the mechanisms that are involved in forming and maintaining some anisotropic trabecular patterns in various mammalian bones. Trabecular patterns or stress trajectories in other femora or femur-like structures (e.g. Culmann's 'crane', Culmann's Fairbairn crane, von Meyer's femur, and Koch's femur) (Figs. 5 and 6) that have played an important role in the origin and/or perpetuation of Wolff's trajectory hypothesis are also evaluated in these comparative contexts. Our intention is to preserve the historical perspective of the often accepted, but inadequately contested, functional analogies drawn between Culmann's crane or cantilevered beam, the additional trajectorial structures, and the actual femora and calcanei. This approach exposes shortcomings of the trajectorial paradigm that have been evasive—only some bones or bone regions subject to specific loading conditions will exhibit what might be considered trajectorial patterns. By design the present study therefore utilized two-dimensional analysis and equations that could have been used by Wolff or his contemporaries. Limitations of using this approach are also discussed and three-dimensional analyses are proposed that will be subsequently conducted on the bones used herein.

We hypothesize that the arched trabecular patterns in adult artiodactyl calcanei (Fig. 4) will correlate with what would be expected if functional bending loads actually mediated their formation along 'tension/compression' trajectories. In this context it is predicted that:

(1) these arched trabecular patterns can be exactly superimposed on the arched tension/compression stress trajectories in mathematically constructed, short, cantilevered beams (Fig. 7), and
(2) the paired quasi-parabolic trabecular tracts in these calcanei and the paired quasi-parabolic stress trajectories in the mathematical beam models will be defined by the same nonlinear equation.

Based on suggestions that the human proximal femur notably differs from a trajectorial structure, we further hypothesize that:

(3) the nonlinear equations that best describe the arched trabecular tracts in the human femoral neck will differ from those that best describe the trabecular tracts in the relatively simply loaded calcanei.
(4) the trabecular tracts in the chimpanzee femoral neck will differ from those in the human femoral neck and those in the chimpanzee will more strongly resemble those in the relatively simple bending models (the calcanei and short cantilevered beams).

In contrast to the femoral neck regions, it is hypothesized that:

(5) the arched trabecular tracts in the trochanteric regions of these two anthropoid femora will have arched trabecular patterns, reflecting adaptations expected in an environment where bending is relatively more prevalent (i.e. symmetric and orthogonal trabecular tracts).

Fig. 5. (A) Culmann's (1866, Fig. 1 of Plate 11) illustration of a Fairbairn type of crane, which is a freestanding, curvilinear tower crane designed by Sir William Fairbairn (see "Fairbairn vignette" in the Appendix A). This type of crane is referred to in Culmann's (1866) text in a chapter with the above illustration (a portion of the original plate), which is attributed to Bessard. But there is evidence that this engineer (or engineering student) did not have an important role in drawing the stress trajectories in the Culmann 'crane' that is illustrated in von Meyer (1867) and Wolff (1870, 1892) (see further discussion in the Appendix A). The tracts indicated with bolded and dashed lines and labeled as 1(a,b), 2(a,b), and 3(a,b) (added here) were used in the present study. The intersection of each curve pair is indicated with a bolded dot. As shown by the inset drawing (added here), θ indicates the locations where angle measurements were made. The trajectories toward the free end of Culmann's 'crane' and the Fairbairn crane are not superimposable (compare Figs. 1 and 5). As argued in the Appendix A, this provides additional evidence suggesting that different engineers (Culmann's students/associates) were involved in the creation of these two drawings. (Modifications made on the original drawing include our addition of the bold and dotted lines and the corresponding symbols.) (B) A Fairbairn crane that can still be seen on the harbor in Bristol, England (reproduced with permission from the original photograph of Alan Goodship, © 2003, All rights reserved).

(A)

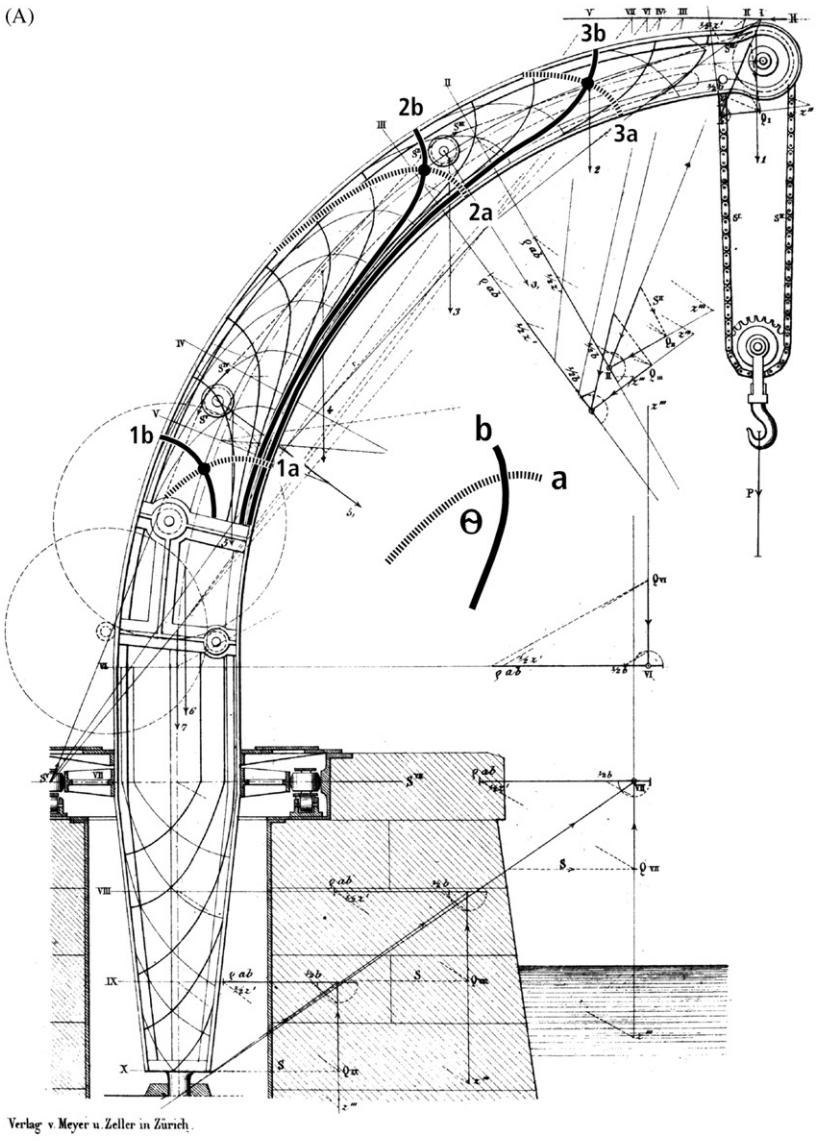

(B)

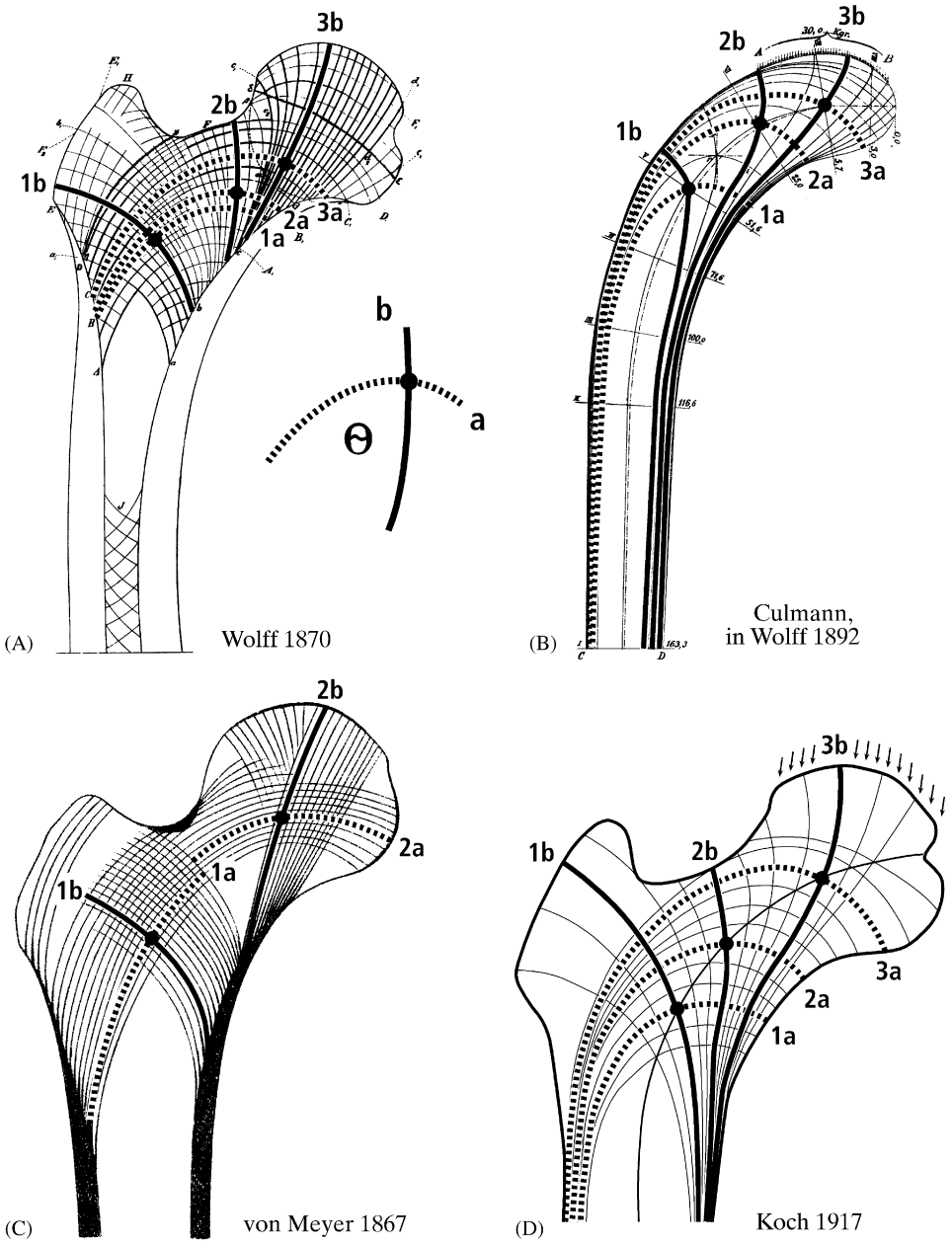

Fig. 6. Some of the trajectorial femora or structures used in the present study. (A) Wolff's (1870) femur; (B) Culmann's 'crane' (from Wolff, 1892); (C) von Meyer's (1876) femur; (D) Koch's (1917, p. 247) femur. Koch used this femur drawing in his mathematical 'confirmation' of Wolff's trajectory hypothesis in the context of stress transfer through this region. Note that there are subtle changes in the 'slope' (as shown by the bolded lines 2b and 3b as they course below the dotted line 2a) of some of the trajectories in Koch's femur. In contrast to the load imposed on the "head" portion of the Culmann 'crane', which is parallel to the longitudinal axis of the fixed end of this structure, the load on Koch's femur course obliquely from the head to the center of the femoral condyles, and represent the vector of the predominant joint force. The trajectories or trabecular tracts that are indicated with bolded and dashed lines and labeled as **1(a,b)**, **2(a,b)**, and/or **3(a,b)** (added here) were used in the present study. As shown by the inset drawing (added here at upper left), θ indicates the locations where angle measurements were made (near or on the mid-axial plane), and the intersection of each pair is indicated with a bolded **dot**.

2. Methods

2.1. Specimen preparation and radiographic analysis

One calcaneus from each of 11 adult male, domesticated sheep (*Ovis aries*; breed is crossed Suffolk/Hampshire and Rambouillet) and 11 adult male, wild Rocky Mountain mule deer (*Odocoileus hemionus hemionus*) were dissected free of soft tissue. The biomechanical 'length' of each bone was measured according to published methods (Skedros et al., 1994), and the "free" and "fixed" ends of the bone were considered to be 0% and 100% of this 'length', respectively (Fig. 4).

One femur was obtained from each of 16 adult modern Caucasian humans (mean age: 47; age range: 19–62; 8 females, 8 males) and 12 adult chimpanzees

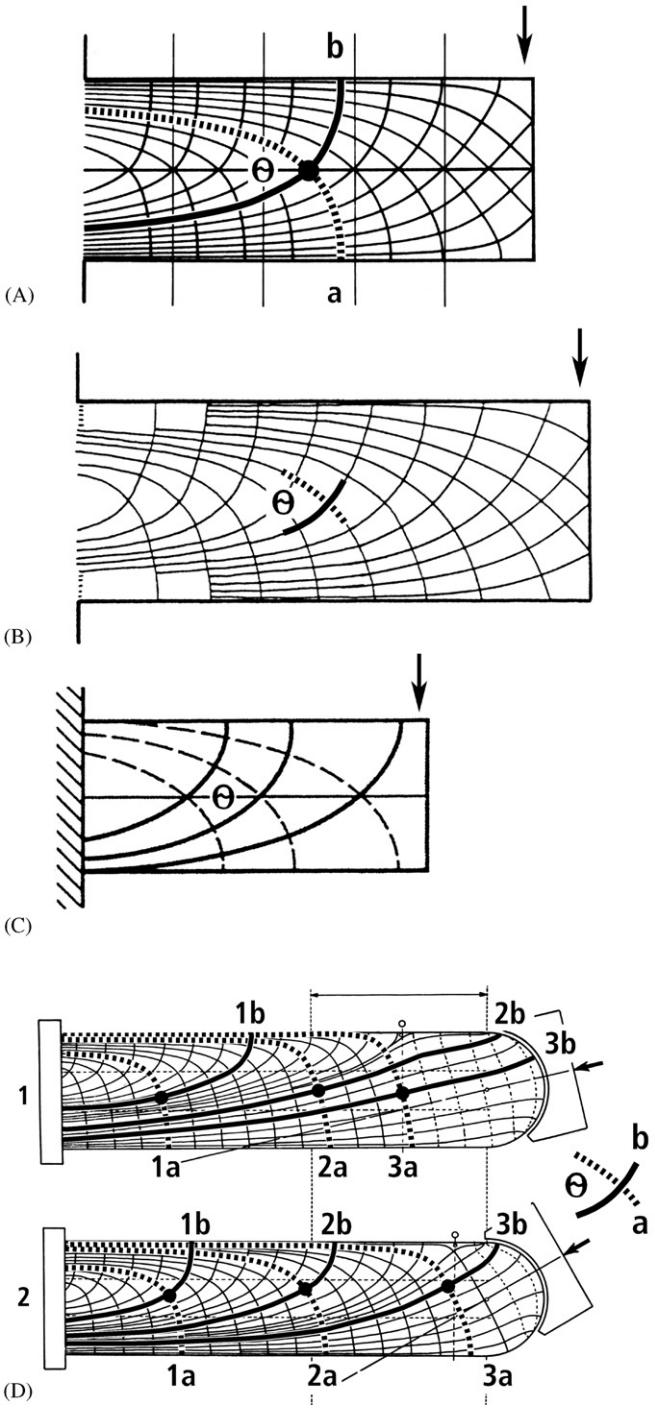

Fig. 7. Cantilevered beams from: (A) Roesler's (1981) paper (reproduced with permission of The American Society of Mechanical Engineers, New York); this beam was used in Roesler's reconstruction of Culmann's 'crane' and is the same beam used by Cowin (2001); (B) Currey's (2002, p. 163) text (reproduced with permission of Princeton University Press, Princeton, New Jersey); (C) Gere and Timoshenko's (1984, p. 318) engineering textbook (reproduced with permission of PWS-Kent Publishing Company, Boston, MA). The two non-orthogonally loaded beams (D 1,2) are from Pauwels' (1976, p. 31) text (reproduced with permission of Springer-Verlag, New York). The trajectories indicated with bolded and dashed lines and marked with **a** or **b** (added here) were used in the present study, and the intersection of the pair of curves is indicated with a bolded **dot.** **θ** indicates the locations where the angle measurements was made.

(*Pan troglodytes*) (age range: 8–39; 5 females, 5 males, 2 unspecified). All human bones were obtained using standard bone-banking techniques (Bloebaum et al., 1993), which included a pre-selection analysis of standardized roentgenograms to ensure that trochanteric and femoral neck trabecular arches (i.e. secondary and principal tensile and compressive groups, respectively) were present in accordance with Singh grade 6 (i.e. had normal appearing bone density and trabecular architecture) (Singh et al., 1970). The chimpanzee bones were from animals that had been kept in large cages with features of natural habitat. None of the humans or chimpanzees had diseases or conditions that affect the musculo-skeletal system. Soft tissues were removed from all bones with manual dissection. External morphologic parameters of all femora were quantified in previous studies (Kuo et al., 1998, 2003); the human femora had normal cervical-diaphyseal (neck-shaft) and anteversion angles. None of the bones had evidence of significant arthritis of the femoral head or condylar regions. The head and neck regions of the chimpanzee and human femora are referred to as the "free" end of these bones (Kuo et al., 1998; Ruff and Hayes, 1984).

Chimpanzee and human proximal femora were radiographed in internal rotation, so that the proximal femur was in neutral (0°) anteversion (Fig. 8). The bone was placed on the film cassette (fine-detail extremity film) (Kodak Ektascan M Film, Eastman Kodak Company, Rochester, New York), supported with modeling clay in the oriented position (Kuo et al., 1998, 2003; Ruff and Hayes, 1983) and the X-ray beam was focused at the base of the neck (anterior-to-posterior projection, 62–69 kV, 4 mAs, and 101.6 cm source-to-cassette distance).

Using the orientation procedures described by Kuo et al. (1998, 2003) and Ruff and Hayes (1984), the proximal aspect of five femora from each species were also radiographed with the posterior condyles flat, which placed the proximal femur in its natural anteversion. Roentgenograms were also obtained after rotating these five bones 5° and 10° in both internal and external rotation (0° rotation is considered the "condyles flat" position). As discussed below, these additional roentgenograms were used to determine potential sources of error in determining trabecular trajectories.

Finally, radiographs were obtained of a 5 mm-thick section, centered on the mid-coronal plane, which was cut from each femur. To make this section, two cuts were made parallel to the mid-coronal plane (each cut was 2.5 mm from the mid-coronal plane) with the femoral neck in neutral anteversion (i.e. the section was made in the plane of the head and neck; hence, with respect to this portion of the proximal femur this section was coronal) (Backman, 1957). As cutting progressed the direction of sectioning was slightly adjusted (externally rotated) in the area of the neck base so that the trochanteric region was also cut in the true coronal plane; this was done to minimize parallax and projection-effect errors when determining trabecular patterns in roentgenograms in this location (Kothari et al.,

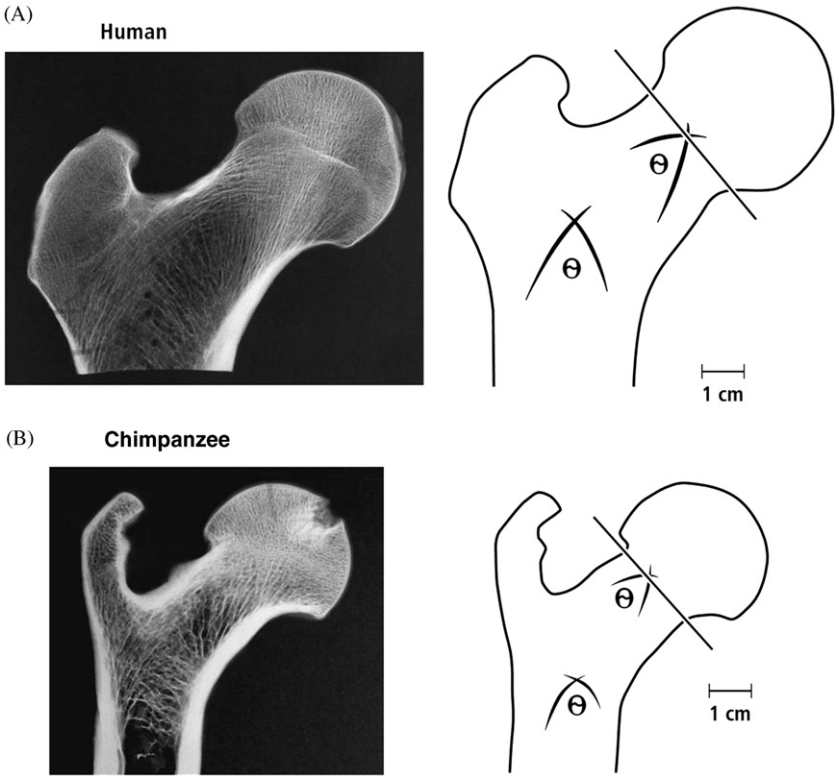

Fig. 8. (A) Anterior-to-posterior roentgenogram of a thin-sectioned human proximal femur used in the present study. The section was made with the bone in internal rotation, which places the proximal femur in neutral (0°) anteversion. The outline drawing of femur on the right shows arched trabecular tracts that were used in the present study. **θ** indicates the locations where angle measurements were made. (B) Anterior-to-posterior roentgenogram of a thin-sectioned chimpanzee proximal femur used in the present study. The section was made with the bone in internal rotation, which places the proximal femur in neutral (0°) anteversion. The outline drawing of femur on the right shows arched trabecular tracts that were used in the present study. **θ** indicates the locations where angle measurements were made.

1998), and also allowed for one complete section from each bone for subsequent radiographic analysis.

Three independent observers, who were blinded to the objectives of the study, examined all roentgenograms of cut *and* un-cut femora to determine: (1) if one or more arched trabecular patterns could be detected in the areas of interest, and (2) if arched trabeculae, when present, exhibited a visually obvious point of intersection at the arch apex. Results of this analysis revealed up to six (50%) chimpanzee bones and three (19%) human bones in which arched and/or intersection trabecular patterns could not be readily detected in roentgenograms of *intact* (un-cut) chimpanzee and human bones. By contrast, there was only one instance (one human bone) where one of the three observers could not detect arched/intersecting tracts in roentgenograms of cut specimens. A pilot study also showed several instances where trabecular arches were not exactly super-imposable in roentgenograms of the same cut and un-cut specimen; this is probably an artifact of overlying cortical and cancellous bone. In view of these findings, and the results of additional error analyses (see below), only roentgenograms of cut bones were used in the subsequent analyses.

Similar comparisons were made between roentgenograms of cut and un-cut calcanei. This was done using 5 mm-thick mid-sagittal sections of contralateral deer and sheep calcanei ($n = 5$ from each species). Each of these calcanei was radiographed (before and after being cut) in the medial-to-lateral projection with the beam focused on 50% bone 'length'. In contrast to the femora, trabecular arches in cut and un-cut calcanei could be exactly superimposed in all cases, and the three independent observers invariably identified arched/intersecting trabecular patterns in roentgenograms of all bones.

As noted, pilot studies were also conducted to establish the margin of error when determining arched trabecular patterns using roentgenograms of the proximal femora in neutral rotation [posterior condyles flat with whole-bone orientation in accordance with Kuo et al. (1998, 2003), and Ruff and Hayes (1983)], and with 5° external rotation and 5° internal rotation. As described above, this analysis was also done to determine whether roentgenograms of whole proximal femora or sectioned proximal femora should be used in the present study. Results showed that the equations (described below) in trochanteric and femoral neck regions that were obtained from $\pm 5^\circ$ rotated, un-cut, whole femora were identical in the corresponding regions of the same bones radiographed in neutral rotation. In contrast, $\pm 10^\circ$ rotation caused changes to occur in several arch pairs in both the human and chimpanzee femora.

These findings suggest that there is an acceptable margin of error ($\pm 5^{\circ}$) when orienting a femoral specimen for radiographing and, hence, subsequent sectioning. This issue may be most relevant in bones with deficient posterior condyles (e.g. arthritic changes) or when only the proximal portion is available (neither of these conditions occurred in the present study).

2.2. Obtaining traces of trajectorial and trabecular arches

One pair of arched intersecting trabeculae in the roentgenograms of each calcaneus and two pairs in each coronally sectioned femur were traced onto a plastic sheet with a fine-point marker. In each femur one pair of trabecular tracts was selected such that their intersection occurred in the region between the mid-neck to sub-capitus (the ''neck region''), and one pair was selected such that its intersection was between the vertical (superior–inferior) distance from the proximal aspect of the calcar femorale to the inferior base of the lesser trochanter (the ''lesser trochanteric region'' or ''trochanteric region'') (Fig. 8). In each calcaneus, one pair of trabecular tracts was selected such that their intersection occurred between 40% and 55% of bone 'length' (Fig. 4).

Tracings of trabecular tracts were made in a darkened room with the assistance of an illuminated view box and magnifying lens. Using tracings magnified $4\times$, the angle (θ) formed at the apex (i.e. intersection) of each paired trabecular arch was also measured to the nearest 1° with a protractor. The angle was determined by drawing, through the intersection of the curves, two straight lines which were perpendicular to the radius of each curve (Koch, 1917, p. 253). Since the curvilinear trabecular ''tracts'' are in reality non-continuous, where even plate-like trabeculae have perforations, care was taken to ensure that each of the selected tracts exhibited at least 90% continuity along its analysed length.

The traced trabecular tracts (two tracts, or ''curves'', in each arched pair) were digitized and assigned Cartesian coordinates (Digitize-Pro 4.1©, Dr. Y. Dannon, Arad, Israel), which were subsequently used to determine the top-five best-fit equations for these data (Table Curve™ 2D v4, Jandel, San Rafael, CA). The resolution of the digitizing program provided 90 points/cm. One of the two curves from each pair was rotated and inverted so that it followed the same course as its paired curve (i.e. could be exactly, or closely, superimposed on the opposing tract). This was done to reduce error associated with the digitization process. Further explanation of this process is given below in the section on axis definitions (see below). Similar tracings and analyses were conducted on paired stress trajectories in analogous regions of the trajectorial structures and bone drawings (Figs. 4–7). In contrast to the orthogonally end-loaded cantilevered beams, two non-orthogonally loaded beams from Pauwels' text (1976) were analysed (Fig. 7D). These beams were included since they might have trajectorial patterns that more closely correspond to the trabecular arches in the femoral necks, which are also typically loaded non-orthogonal to the neck axis.

In the orthogonally loaded beams, only the stress trajectories of Roesler were examined. This is because the stress trajectories in Roesler's beam can be *exactly* superimposed on the trajectories of *all* of the other orthogonally loaded beams (Fig. 7B and C). Tracings of arched trabecular tracts in each calcaneus and femur were examined to determine if they could be exactly, or inexactly, superimposed on the stress trajectories of Roesler's cantilevered beams. In the calcanei the percentage of bone 'length' where the trabecular tracts intersect was compared to trajectories that intersected at an equivalent percent length of Roesler's cantilevered beam.

2.3. Trajectorial analysis: axis definitions and digitization process

The procedure used to reliably obtain a best-fit equation for a curve encompasses at least 8 steps (Fig. 9). Once the desired intersecting arches are traced, they are enlarged $2\times$ (step 1). After being traced and enlarged, the shorter, post-intersection portion of the curves [i.e. the ''short tails'' cranial (femora) or distal (calcanei) aspect to intersection)] are identified. The post-intersection portions are then measured from the intersection to their respective ends using a pliable wire (step 2). The shorter of the two post-intersection 'tails' is determined and its arc length measured. A corresponding length is measured onto the longer post-intersection tail and marked (step 3). A line is then drawn from the tip of the shorter post-intersection tail to the equal arc length mark on the longer post-intersection tail (step 4). The ''x''-axis is then drawn as a line passing though the arch intersection (0,0) and forming a 90° angle with the line joining the two short tails (step 5). The y-axis is drawn as a perpendicular to the x-axis at the arch intersection (step 6). If all is done correctly the y-axis should be parallel to the line joining the post-intersection curves and should traverse the arch intersection.

To insure consistency when digitizing the curves, the positive segment of the x-axis is defined as the distance between the y-axis and the line connecting the short tails. The positive y-axis extends the same distance toward the long tail of the arch that is being digitized (step 7). Our pilot studies demonstrated that this reduces operator error in the digitization process and reliably produces a best-fit equation despite potential differences in arch orientation. To make these axis definitions the same for all curves, tracings of the other curve of each pair were inverted and rotated in order to make both curves fit the same axis definitions (step 8). In some trajectorial femora (e.g. Koch's femur drawing, Fig. 6) there are trajectories that have obvious changes in 'slope' (e.g. from concave to convex or vice versa) along their length. In this instance measurements were only made on the curve extending from the superior (cranial) aspect (toward the capitus femoris) to the

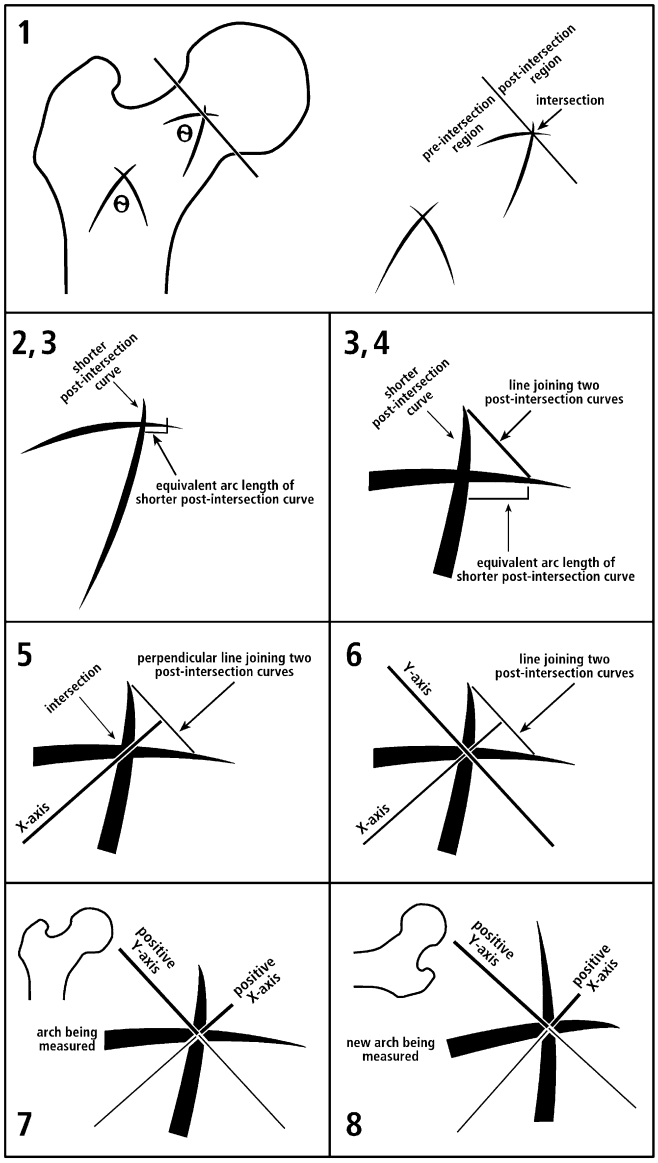

Fig. 9. Eight steps used for axis definitions; see text for descriptions.

approximate point at which this change in slope occurred. The selection of a portion of these curves helps to provide reliable and consistent data for regions of the curve in the area of interest. The present study only deals with the trabecular or trajectorial arches near the arch intersection; therefore, the infrequent distal changes in slope—which only occurred in some trajectorial drawings—were ignored.

Because of the longer lengths of hypothetical trajectories in the femora compared to the traceable trabecular arches in the actual femora, the trajectories were not traced from end to end. Instead, the length of the shortest post intersection tail (which was always at the superior aspect of the arch in the 'trajectorial' femora) was determined and a distance $2\times$ of that was mapped onto the longer tail of the curve. This ensured that the lengths of trajectories in these structures were more comparable to the traceable length of trabecular curves in the actual bones. This procedure was followed in all cases except for trajectories 1a and 3a of Koch's 'trajectorial' femur and 2a in von Meyer's femur (Fig. 6) in which a distance of only $1\times$ the shortest short tail was used. The selected arches in the lateral aspect of the trochanteric region of von Meyer's femur also required a slight modification in the tracing process. Because these trajectories extend from the lateral intertrochanteric region to the peripheral margins of the femoral head, the superior "end" of these trajectories was considered to be the most medial trochanteric trajectory.

2.4. Additional sources of error and clarifications

Pilot studies showed that nearly identical equations were obtained for all curves in calcanei and beams, but a variety of equations were frequent in the human femora. For example, in pilot studies the equation $y^{-1} = a + b/x$ was the most prevalent equation and seemed to best fit most trabecular curves in the human bones. The congruence of the curvilinear trabecular or trajectorial tracts and their fit to this equation becomes clear on gross observation—these curves fit only a region of the curve (Fig. 10B). The observation that a traced curve fits a portion of a larger or more complex curve and that the same traced region can fit other equations with very little manipulation raises important questions about the limitations of the methods used in this study. Strict axis definitions and tracing procedures (steps 1–8, above) need to be followed in order to produce a consistent equation describing curves that closely fit the tracings. Despite rigorous axis definition and tracing procedures, the Table Curve^{TM} program at times supplied the exponential equation $y = a + b^{(-x/c)}$ as the best fit for the traced curve. This exponential equation and the equation $y^{-1} = a + b/x$ describe functions that are very different. They are similar, however, in a small region that corresponds to the trabecular curves (Fig. 10). Unless strict axis definition procedures are followed these equations are assigned interchangeably.

Pilot studies revealed that among the myriad equations in the Table Curve^{TM} program, the "simple equations menu" was most optimal for distinguishing differences between curves within one bone or structure. The simple equations menu also provided comparable data and a clear distinction between dissimilar curves. Other equation menus that were studied contained polynomial, rational, and curve-fit kinetic equations that produced many equations that fit many curves better than $r^2 = 0.99$. However, in most cases these curves were bizarre and/or complexly non-monotonic. Polynomial equations were only exclusively used in one instance (curve fitting in Pauwels' beams) where the "simple equations menu" equations simply could not provide a close fit ($r^2 < 0.90$). In all cases, all curve fits were visually examined to insure that they: (1) closely fit the graphical plot, and (2) had a very high coefficient of determination (typically $r^2 > 0.97$). Additionally, plots of the residual errors were also examined to ensure that in all cases the curvilinear

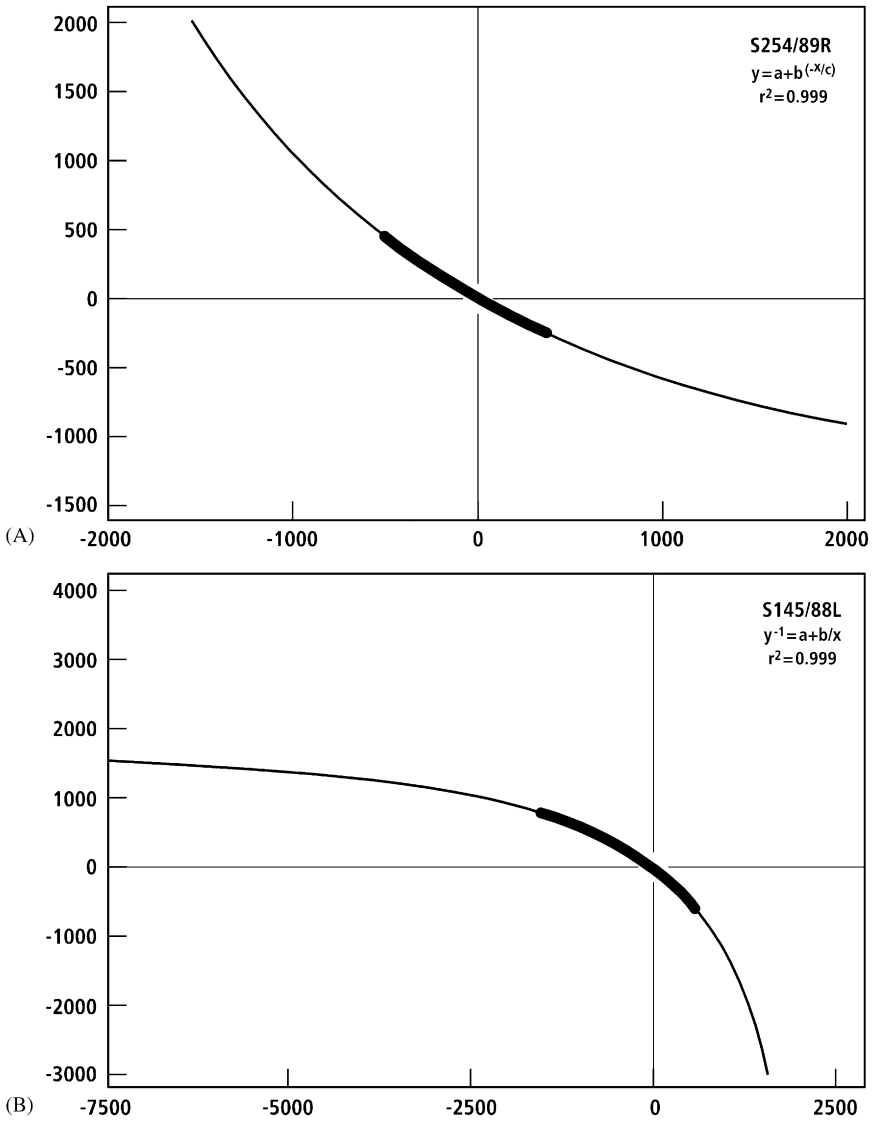

Fig. 10. Curve fits for the two most-common equations for the traced trabecular tracts obtained from human femoral neck regions. The darkened portion of each curve represents the length of the traced trabecular tract. The equations are: (A) $y = a + b^{(-x/c)}$, (B) $y^{-1} = a + b/x$.

relationship between x and y variables did not violate homoscedasticity assumptions (Kachigan 1986). Use of the simple equations menu also helped to avoid the assignment of erroneous equations, whilst producing comparable functions that clearly fit the traced curve.

To ensure that our methods reliably produced consistent equations, $\pm 5^\circ$ and $\pm 10^\circ$ axis rotations in both the clockwise and counterclockwise directions were also performed on traced trabecular arches in three deer calcanei, three sheep calcanei, three human femora (trochanteric and femoral neck) and three chimpanzee femora (trochanteric and femoral neck). All axis definition requirements were followed (*steps 1–8*) with the exception of the final axis being rotated 5° and 10° in both the clockwise and counterclockwise direction. Therefore, the "origin" (0,0) of intersection remained the same while the axis was rotated. The 5° rotations produced the same equations that had been originally assigned to the curves for all bones. In contrast, 10° rotations produced a different equation in one superior trabecular tract in a human femoral neck. Upon gross examination, the equation produced by the rotations of this one curve clearly did not fit. This exception is a result of the greater length of trabecular arches in the superior aspect of the femoral neck region. When this trabecular tract was measured from its proximal tip to an arc length of only $2\times$ that of the short tail, the equation is the same as that obtained without rotation. As shown by this result, the best-fit curve that results after 10° rotation is not expected and is attributable to a large portion of a curving "long tail". These results demonstrate that $\pm 5^\circ$, which is within our assessment of intra- and inter-observer error, is associated with an acceptable margin of error for determining the axes using definitions in steps 1–8.

2.5. Statistical analyses for paired comparisons

A one-way ANOVA design was used to evaluate comparisons of trabecular tract intersection angles. The level of statistical significance was considered to be $p \leqslant 0.05$.

3. Results

Calcanei (Tables 1 and 2): All calcanei showed the presence of obvious arched trabecular tracts (Fig. 4). Supporting hypotheses 1 and 2, the dorsal (''compression'') and plantar (''tension'') trabecular tracts of all sheep and deer calcanei could be exactly superimposed on trajectories in Roesler's beam at proportionally similar percentages of diaphyseal or beam 'length' (Figs. 4 and 7A). In turn, the arched trabecular patterns in the calcanei and the stress trajectories of the cantilevered beams can be described by the same nonlinear equation ($y^{-1} = a + b/x$, Table 1). Only one curve obtained from a plantar calcaneal tract exhibited a relatively lower r^2 value (< 0.97).

Trabecular tract intersections in the calcanei are typically orthogonal to quasi-orthogonal ($90^\circ + 7^\circ$; range: 70°–102°), with $90^\circ + 5^\circ$ in 76% of arches and exactly 90° in 33% of arches (Table 2).

Human femora (Table 2): In all cases, the three independent observers recognized arched trabecular patterns and intersections in the neck of each of the (thin sectioned) human femora. However, there were two bones where one of the three investigators could not identify trabecular arch *intersections* in the trochanteric region. In 62.5% (10/16) of the human femoral necks, the nonlinear equations describing the inferior trabecular tracts are different from the nonlinear equations describing the trabecular tracts in the calcanei and the stress trajectories in the cantilevered beams (Table 2). Also in support of hypothesis 3, trabecular tract intersections in the human femoral necks were non-orthogonal, and these tracts also had shapes that often differed from the trabecular tracts in the calcanei and the stress trajectories in the simply loaded beams. The superior aspect of the human femoral neck varied only once (1/16) when compared to these simply loaded structures. In the human bones there were three curves (3/78) where the r^2 value was less than 0.97 (all three curves are from the superior (''tension'') tracts of the femoral necks); in these cases high-order polynomial functions provided a better fit of the data.

In support of hypothesis 5, all of the medial and lateral trabecular tracts in the human trochanteric region best fit the same equation that best fit the trajectories in the beams. Additionally in support of hypotheses 3 and 5, respectively, trabecular intersections in the human proximal femora are typically non-orthogonal in the neck ($69^\circ \pm 12^\circ$; range: 51–90°) and typically quasi-orthogonal in the trochanteric region ($92^\circ \pm 6^\circ$; range: 82–105°) ($p < 0.0001$).

Chimpanzee femora (Table 2): In all cases, the three independent observers recognized arched trabecular patterns *and* intersections in the neck and trochanteric regions of each of the (thin sectioned) chimpanzee femora. In 83.3% (10/12) of the chimpanzee femoral necks, the nonlinear equations describing the inferior trabecular tracts differed from the nonlinear equations describing the trabecular tracts in the calcanei and the stress trajectories in the cantilevered beams (Table 2). In contrast, the superior tracts in the chimpanzee femoral neck never varied when compared to these simply loaded structures. In the chimpanzee femora there were four curves (4/48) where the r^2 value was less than 0.97 (three curves in the trochanteric region and one in the superior femoral neck); in these cases high-order polynomial functions provided a better fit of the data.

In all but one chimpanzee bone (i.e. a medial trochanteric tract) the trabecular tracts from the medial *and* lateral trochanteric region matched the equations for the cantilevered beams. Trabecular intersections in the chimpanzees are typically non-orthogonal in the femoral neck ($70^\circ \pm 12^\circ$; range: 45–85°) and obtuse in the trochanteric region ($117^\circ \pm 10^\circ$; range: 100–132°) ($p < 0.001$); these findings do not support hypotheses 4 and 5, respectively.

Table 1
Comparisons of best-fit equations for trajectories in: (A) beams, (B) calcanei, and (C) cranes

Trajectorial structures	Mean r^2 values (range)	Mean intersection angles	Equations	
			$y^{-1} = a + b/x$	$y = a + b^{(-x/c)}$
A. Beams				
Roesler's cantilevered beam	0.993 (0.986–0.999)	90°	100%	0%
Pauwels' cantilevered beam	0.945 (0.757–0.999)	90°	100%	0%
B. Calcanei				
Deer calcanei	0.993 (0.954–0.999)	$89^\circ \pm 8^\circ$	100%	0%
Sheep calcanei	0.995 (0.984–0.999)	$90^\circ \pm 6^\circ$	100%	0%
C. Cranes				
Culmann's 'crane'	0.961 (0.878–0.999)	88°*	100%	0%
Fairbairn crane	0.990 (0.978–0.999)	90°	100%	0%

*The intersections are 90° in two locations and 84° in one location (Fig. 4). These data show that trajectories in Roesler's beam (Fig. 7A) can be described by the same equations for trabecular tracts in the calcanei, trajectories in one of Pauwels' non-orthogonally loaded beams (Fig. 7, D2), and the Fairbairn crane and Culmann 'crane' (Figs. 3, 5, and 6).

Table 2
Trabecular tract best-fit equations and intersection angles of: (A) human and chimpanzee femora, and (B) sheep and deer calcanei

A. Femora				
Human femora	Femoral neck		Lesser trochanter	
Equations	Superior	Inferior	Lateral	Medial
$y^{-1} = a + b/x$	93.8%	37.5%	100.0%	100.0%
$y = a + b^{(-x/c)}$	6.2%	56.3%	0.0%	0.0%
$y = a + bx$	0.0%	6.2%	0.0%	0.0%
Mean angle of intersection	$69° \pm 12°$		$92° \pm 6°$	
Range of angles of intersection	51°–90°		82°–105°	
Chimp femora	Femoral neck		Lesser trochanter	
Equations	Superior	Inferior	Lateral	Medial
$y^{-1} = a + b/x$	100.0%	16.7%	100.0%	91.7%
$y = a + b^{(-x/c)}$	0.0%	83.3%	0.0%	0.0%
$y = a + bx$	0.0%	0.0%	0.0%	8.3%
Mean angle of intersection	$70° \pm 12°$		$117° \pm 10°$	
Range of angles of intersection	48°–85°		100°–132°	
B. Calcanei				
Sheep calcanei				
Equations	Dorsal	Plantar		
	100.0%	100.0%		
	0.0%	0.0%		
$y = a + bx$	0.0%	0.0%		
Mean angle of intersection	$90° \pm 6°$			
Range of angles of intersection	76°–102°			
Deer calcanei				
Equations	Dorsal	Plantar		
$y^{-1} = a + b/x$	100.0%	100.0%		
$y = a + b^{(-x/c)}$	0.0%	0.0%		
$y = a + bx$	0.0%	0.0%		
Mean angle of intersection	$89° \pm 8°$			
Range of angles of intersection	70°–100°			

Human and chimpanzee femora comparisons: Statistical comparisons of intersection angles between chimpanzees and humans showed the following results: (1) $p = 0.003$ for chimpanzee trochanteric vs. human trochanteric, and (2) $p = 0.8$ for chimpanzee femoral neck vs. human femoral neck.

3.1. von Meyer's femur, trajectorial femora, and "cranes" (Tables 2 and 3)

Nearly all of the 'trajectories' analysed in von Meyer's (1867), Wolff's (1870), and Koch's (1917) femora best fit the same nonlinear equation in the calcanei. The only exceptions were the trajectories in the inferior neck region of von Meyer's drawing (Fig. 6). Equations in this region matched those that best fit the chimpanzee and human inferior femoral neck trabecular tracts. Trajectorial intersection angles were generally orthogonal except in von Meyer's femur where a mean of 73° was observed, which is similar to the values found in the actual femora (Tables 2 and 3). The r^2 values are much lower in Koch's (0.927) and Wolff's (0.974) femora (compared to von Meyer's at 0.982). Plots of residual errors also showed greater amplitudes of the residuals in these cases. These lower r^2 values are a result of subtle curvature changes in the longer trajectories. The curve fits in these two trajectorial femora improved when only the central portions of the trajectories were traced.

All trajectories analysed in both Culmann's 'crane' and the Fairbairn crane best fit the same nonlinear equation that best fit the trabecular curves in the calcanei (Table 1). However, the trajectories in the Fairbairn crane had notably higher r^2 values than those in the Culmann 'crane' (e.g. mean values: 0.990 vs. 0.961, respectively). The r^2 values were typically lower when compared to the human and chimpanzee femora, which is the consequence of a

Table 3
Trajectorial femora: equations and intersection angles. (A) Wolff's femur, (B) Koch's femur, and (C) von Meyer's femur

A. Wolff's femur	Femoral head		Femoral neck		Lesser trochanter	
Equations	Superior	Inferior	Superior	Inferior	Lateral	Medial
$y^{-1}=a+b/x$	100%	100%	100%	100%	100%	100%
$y=a+b^{(-x/c)}$	0%	0%	0%	0%	0%	0%
$y=a+bx$	0%	0%	0%	0%	0%	0%
Intersection angle	90°		90°		90°	
B. Koch's femur	Femoral head		Femoral neck		Lesser trochanter	
Equations	Superior	Inferior	Superior	Inferior	Lateral	Medial
$y^{-1}=a+b/x$	100%	100%	100%	100%	100%	100%
$y=a+b^{(-x/c)}$	0%	0%	0%	0%	0%	0%
$y=a+bx$	0%	0%	0%	0%	0%	0%
Intersection angle	90°		90°		90°	
C. von Meyer's femur	Femoral neck		Lesser trochanter			
Equations	Superior	Inferior	Lateral	Medial		
$y^{-1}=a+b/x$	100%	0%	100%	100%		
$y=a+b^{(-x/c)}$	0%	100%	0%	0%		
$y=a+bx$	0%	0%	0%	0%		
Intersection angle	69°	77°				

greater length of the trajectories. Plots of residual errors also showed greater amplitudes of the residuals in these cases. The trajectories in the Fairbairn crane intersected at 90°, while some of the trajectories in Culmann's 'crane' intersected at ~84°.

3.2. Cantilevered beams

All trajectories analysed in Roesler's cantilevered beam best fit the same nonlinear equations for the calcanei with an r^2 value > 0.986 ($y^{-1}=a+b/x$, Table 1). The intersections in Roesler's beam were also invariably orthogonal.

Although all the trajectories measured in Pauwels' two non-orthogonally loaded cantilevered beams formed 90° intersections (Fig. 7), the r^2 values were typically lower ($r^2<0.945$) when they were fit to either of the two most common equations used in the calcanei and femora. High-order polynomial equations were required for achieving fits of $r^2>0.97$ for the trajectories analysed in Pauwels' beams.

4. Discussion

4.1. Trabecular patterns in the human femoral neck are clearly not trajectorial

Results in the sheep and deer calcanei showed that the same nonlinear equation invariably best fit their dorsal ("compression") and plantar ("tension") trabecular tracts, and that these tracts could be superimposed on the corresponding mathematically derived compression and tension stress trajectories of the simply loaded cantilevered beams. Additionally, the opposing calcaneal trabecular tracts typically formed orthogonal to quasi-orthogonal intersections. In contrast, trabecular tracts in the human femoral necks were non-orthogonal, and also had shapes that often differed from the trabecular tracts in the calcanei and the stress trajectories in the simply loaded beams. However, the trabecular tracts in the chimpanzee femoral neck were also non-orthogonal, resembling those in the human femoral neck. These results suggest that the trabecular patterns in the calcanei satisfy basic tenets of the trajectorial hypothesis, while those in these anthropoid femoral necks do not. As discussed below, it is suggested that, in contrast to the calcanei and simple beams, the anthropoid femoral necks deviate significantly from the trajectorial paradigm since they receive relatively prevalent shear stresses, which are best accommodated by non-orthogonal trabecular tracts. We also consider the possibilities that asymmetrical trabecular patterns in these proximal femora may reflect the different developmental 'fields' (trochanteric vs. neck vs. head) that formed these regions—of which there is no parallel in the calcanei.

In the human femoral neck, the trabecular tracts exhibited acute (mean ± SD: 69° ± 12°) intersections. Similar acute intersections are depicted in von Meyer's anatomical drawing of a proximal femur but not in the trajectories of Culmann's 'crane', the Fairbairn crane, or the theoretical trajectorial/trabecular patterns in Koch's and Wolff's femur. Based on similar observations of this non-orthogonal construction in actual human femora, past

and recent investigations have also questioned the conception of the human proximal femur as a trajectorial structure. For example, in computational analyses Carter, Jacobs, and co-workers (Jacobs et al., 1997) calculated magnitudes of normal stresses in various locations throughout a two-dimensional model of a mid-coronally sectioned human proximal femur. Using a nonlinear weighting scheme, they determined the orientation of trabecular tracts in these locations, and noted that one consequence of this "time-averaged" principal stress construction (which they state is similar to Wolff's principal stress concept if there is no variation in direction of cyclically applied loads) is that it becomes possible to "…form cancellous bone tracts with principal orientations that are not perpendicular to each other" (Carter and Beaupré, 2001, p. 149). Additionally, using simulated loading imparted to a two-dimensional mid-coronal slice through the human proximal femur, Carter, Beaupré and co-workers showed that the "arcuate system of trabeculae"[4] experiences *both* tension and compression stresses along the principal orientation of the trabeculae, and "…the predicted orientations of trabecular architecture throughout the proximal femur match the early drawings of von Meyer [1867]" (Beaupré et al., 1990; Carter and Beaupré, 2001, p. 152). As noted, and discussed further below, the finite element analysis of Pidaparti and Turner (1997) suggests that these non-orthogonal intersections in the human femoral neck may represent adaptation for shear stresses engendered by prevalent complex/torsional loading—Wolff's trajectorial paradigm does not include shear as an important mechanical correlate of trabecular architectural anisotropy.

Neck vs. trochanteric trajectories: In contrast to those of the human femoral neck, the trabecular tracts in the human trochanteric region often closely resembled the orthogonally intersecting trabecular tracts in the calcanei and the stress trajectories in the beams (Fig. 8, Tables 1–3). In the context of Wolff's trajectorial paradigm, orthogonally intersecting trabeculae correlate with a medial-to-lateral bending moment in this region of the human femur. However, in the presumably similarly loaded chimpanzee trochanteric region the trabecular tracts typically formed obtuse intersections ($117^\circ \pm 10^\circ$). This unexpected architectural arrangement is difficult to reconcile in a simple mechanical context. This architecture also seems inconsistent with predominant collagen fiber orientation data in cortical bone suggesting that the chimpanzee neck, and hence the proximal diaphysis with which it is continuous,

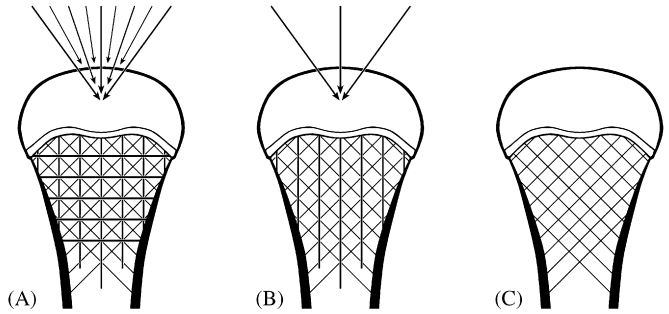

Fig. 11. Heřt's (1992) model of cancellous bone trabeculae in alternating loading by vertical and oblique forces (A). According to Heřt the stress placed on oblique trabeculae by an oblique force exceeds the strain placed on vertical trabeculae by an axial force (B). Trabecular modeling (i.e. mini-modeling) results in a pattern of the two intersection systems oriented in two oblique directions (C). In Heřt's view this accounts for the quasi-parabolic, non-orthogonal intersections in the human femoral neck region (Fig. 12). (Re-drawn from Heřt (1994) with permission of the publisher, Elsevier Science, New York).

receives relatively more prevalent *bending* than the human femoral neck (Kalmey and Lovejoy, 2002; Lovejoy, 2005).[5] In the chimpanzee trochanteric region, a structure/function relationship between habitual loading and obtuse trabecular intersections might be clarified by considering Heřt's (Heřt, 1992, 1994) functional interpretation of predominant trabecular patterns.

Heřt (1992, 1994) suggests that in a metaphyseal/epiphyseal region of a weight-bearing bone, such as the human femur, the trabeculae form "paired" oblique angles, where each principal tract corresponds to the *compressive* predominant joint load vectors near the *extremes* of a typical range of joint excursion. In turn, these oblique trabecular tracts may appear as quasi-parabolic arches. This interpretation precludes an important role for *tension* trajectories (Figs. 11 and 12). In this context the formation of obtuse trochanter intersections in chimpanzees may then be strongly influenced by extremes of predominant load vectors produced by their Trendelenburg-type gait patterns (Elftman and Manter, 1935; Jenkins, 1972; Kalmey and Lovejoy, 2002; Lovejoy, 2005). In contrast to humans, chimpanzees habitually shift their center of mass of the head, arm, and trunk laterally (over the supporting limb) (i.e. Trendelenburg gait) in order to achieve equilibrium during single-leg support phase (Lovejoy, 2005). As noted by Kalmey and Lovejoy (2002), this gait pattern occurs because non-human primates (including hominoids) lack a specialized abductor apparatus (gluteus minimus and medius, pyriformis, etc.) that minimizes pelvic drop, which

[4]Carter and Beaupré (2001, p. 150) designate the inferior trabecular tract as the "compression trabecular tract", and state that the superior ("tension") trabecular tract is a "…secondary "arcuate" system of trabeculae [that] arches from the infero-medial joint surface through the superior neck and into the lateral metaphyseal region." Previous investigators and authors have used similar designations that minimize bias favoring the trajectory hypothesis (Carey, 1929; Elke et al., 1995; Farkas et al., 1948; Heřt et al., 2001; Kapandji, 1987; Trueta, 1968; Viola, 2002).

[5]In cortical bone, predominant collagen fiber orientation (CFO) is a material characteristic that has high reliability for reflecting adaptation for the presence of a habitual strain mode (e.g., tension vs. compression) between locations of the same bone cross-section (Mason et al., 1995; Skedros et al., 2004; Bromage et al., 2003; Skedros, 2001). Consequently, predominant CFO can help interpret load history in cortices of bone regions where it may be difficult or impossible to obtain in vivo strain data.

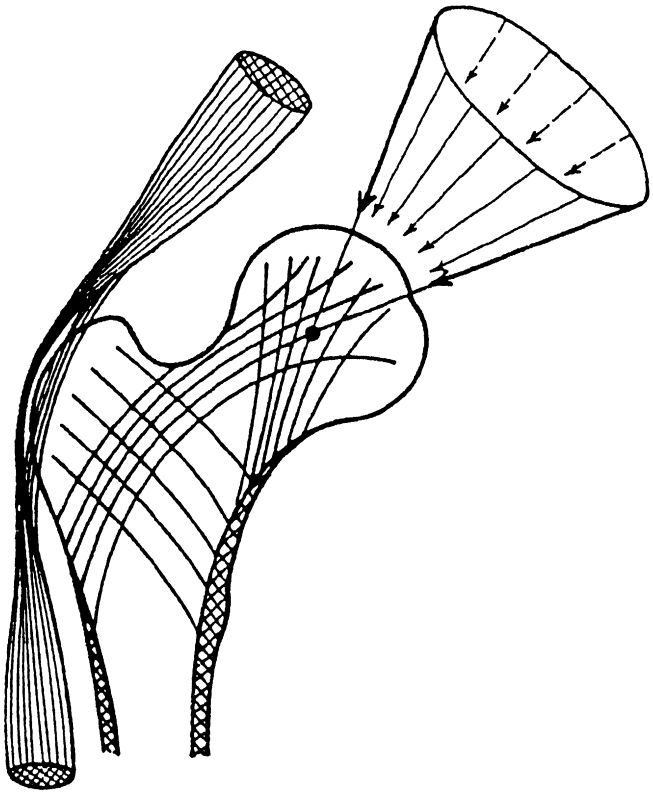

Fig. 12. Heřt's (1992) drawing of a human proximal femur. The original figure legend reads: Interpretation of the architecture of the spongiosa at the upper end of the femur. The two principal trabecular systems in the neck are exposed to pressure [compression]. Their direction corresponds to the marginal force of the fan of resultant forces acting on the articular end of the bone. Two trabecular systems are developing in the apophysis—a tension system oriented in the direction of the inserting muscles and a pressure system resulting from pressure of the apophysis against the diaphysis. (Reproduced from Heřt (1994) with permission of the publisher, Elsevier Science, New York).

is especially pronounced during bipedal locomotion. Although bipedal gait is relatively uncommon in chimpanzees (Alexander, 2004; D'Aout et al., 2004; Schmitt, 2003; Thorpe et al., 1999), their typical ambulatory activities also incur significant pitching of the trunk (with bent hip and bent knee) that, compared to humans, significantly increases the range of joint load vectors (hence stress trajectories) across the hip (Jenkins, 1972; Martinón-Torres, 2003; McHenry, 1975).

Even if a broad range of stress trajectories explains the existence of obtuse intersections in the chimpanzee trochanteric region, it is not clear why acute, not obtuse, intersections occur in the chimpanzee femoral neck. Assuming that predominant trabecular orientations reflect habitual loading patterns, these obtuse intersections in the trochanteric region may represent an 'atypical' manifestation of shear-related adaptation (discussed below). Alternatively, and in view of Heřt's interpretation of the mechanical relevance of anisotropic trabecular architecture, we suggest that these obtuse intersections reflect the extremes of a broad range of stress trajectories, which in chimpanzees is relatively broader in more distal femoral regions as a function of length of the effective lever arm across the hip (i.e. greater in the trochanteric region than in the neck). Thus, compared to the chimpanzee trochanteric region, the chimpanzee femoral neck experiences a relatively more restricted range of joint load vectors such as illustrated in Fig. 12. Support for this interpretation is also consistent with suggestions of Miller et al. (2002) who simulated trabecular orientations in a two-dimensional finite element model of a human proximal femur subject to various loading directions. They concluded that the alignments of the 'secondary tensile group' and 'secondary compressive group' of trabeculae (i.e. those in the trochanteric area) are "…determined mainly by the extreme load cases …which cause large bending moments in the femur. Thus trabecular directions in different zones [i.e. neck vs. trochanteric regions] are determined by different load cases."

4.2. *The 'adaptability' and biomechanics of cancellous bone: do non-orthogonal femoral neck arches reflect "shear-priority" adaptations?*

In a review of the literature on trabecular bone mechanical properties, Keaveny (2001, pp. 16–2) states that "The strength of trabecular bone depends on volume fraction,[6] architecture [e.g. trabecular orientation, thickness, and connectivity], and the tissue material properties, in that order of importance." Ford and Keaveny (1996) further point out that "…shear may be a dominant failure mode during off-axis loading of trabecular bone in vivo,…" These facts are relevant in the context of functional adaptation of the anthropoid hip since this region is habitually loaded "off axis" (e.g. in humans, loading is typically ~22–37° superior to the femoral neck axis) (Bergmann et al., 1993; Davy et al., 1988). Hence, it seems that the anthropoid femoral neck especially in the human hip (because of the relatively long femoral neck), would be in a precarious situation without functional adaptations that accommodate prevalent/predominant shear produced by the habitual co-existence of bending and torsion. Specific functional adaptations for shear are expected in this region because experimental data have shown that, when tested to failure in tension, compression, and shear, trabecular bone is notably weakest in shear (Ford and Keaveny, 1996; Keaveny and Hayes, 1993; Keaveny et al., 2001, 1994) (Fig. 13).

In view of this disparity, we invoke the idea that shear loads, which are minimally considered in the Wolffian paradigm, are important considerations for interpreting adaptation of trabecular architecture. Experimental studies

[6]Elastic modulus (stiffness) and failure stress of cancellous bone depends primarily on apparent density (the product of volume fraction and bone tissue density, the latter being essentially constant at about 2 g/cm^3) (Keaveny et al., 2001).

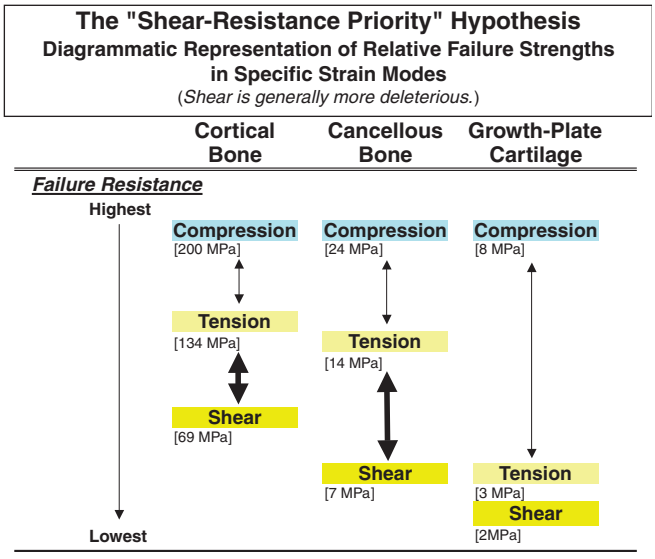

Fig. 13. Diagrammatic representation of the "shear-resistance priority hypothesis". This shows that cortical and cancellous bone types are disproportionately weaker in shear than in tension or compression (increased vertical separation in the diagram). Although the disparity in cartilage is less marked, cartilage has poor tensile and shear strength. This suggests that tension and shear are important in driving the ontogenetic adaptation of these tissue types.

Note: that the disparity (**thick double-headed arrows**) between tension and shear is broader in cancellous bone than in cortical bone. With the cortical and cancellous bone types, the disparity between compression and tension (**thinner double-headed arrows**) is less marked.
The absolute failure strengths and differences shown above between the tissue types are not directly comparable.

Values were obtained from these sources:
Cortical bone: Cowin (1989a) for human bone; Values for bovine bone include: compression 197 MPa, tension 130 MPa, and shear 70 MPa.
Cancellous bone: Estimated from Keaveny et al. (2001) for bovine bone using strength anisotropy ratios (longitudinal/transverse strength) and volume fractions between 0.3 and 0.5.
Cartilage: The compression value is estimated from human articular cartilage (Yamada, 1970); the values for tension and shear are from bovine tibia growth plates (Williams et al., 1999, 2001).

of Keaveny and co-workers (Keaveny, 2001) have contributed most significantly to the development of the idea that shear loads—by being potentially more deleterious than tension or compression loads—may have "priority" among these naturally selective stimuli in affecting the emergence of developmental adaptations in cancellous bone. This hypothesis is also supported by experimental data showing differences in microdamage accumulation in trabecular bone when loaded "on-axis" in compression vs. "off-axis" in shear (Wang and Niebur, 2006), and studies suggesting that shear loads are important in the etiology of osteoporosis-related fragility fractures of the proximal femur (Greenspan et al., 1998; Pinilla et al., 1996) and vertebral bodies (Myers and Wilson, 1997). At the tissue/cellular level, shear can also be distinguished from other strain modes by differences in deformation of the cell body or by evoking different biophysical stimuli (e.g. streaming potentials or fluid-flow dynamics) (Carter and Wong, 1988; Judex et al., 1997; Rubin et al., 1996).

Additional observations supporting the idea that prevalent/predominant shear loads have "priority" over tension and compression in producing developmental adaptation also include yield stress data for bovine tibial trabecular bone loaded in longitudinal vs. transverse directions, and their strength anisotropy ratio (SAR) data, plotted as a function of apparent density for three different loading modes (compression, tension, shear) (Keaveny et al., 2001). These data, shown as curves in Fig. 14, demonstrate that strength (dashed lines) always increases with increasing volume fraction and depends critically on loading direction and mode. Furthermore, the strength anisotropy ratio varies from 2 to 10; it depends on volume fraction and loading mode, being greatest for compression and *least for shear*. Hence, trabecular *orientation* may have a relatively greater influence on trabecular bone strength when loaded in prevalent/predominant *shear*. In view of these data, we suggest that regional modifications in volume fraction are *not* sufficient for accommodating the shear stresses that are common in the proximal femur. Consequently, if the non-orthogonal trabecular intersections are adaptive in the anthropoid femoral necks examined in this study, then it is plausible that they are configured in ways that ultimately help accommodate shear stresses in this region. This is consistent with results of the finite element analysis of Pidaparti and Turner (1997, p. 981) (see also Fernandes et al., 1999).

> Our analyses show that non-orthogonal trabecular orientations [in the human femoral neck] reduce shear coupling under multiaxial loading, e.g. bone near a synovial joint, but under predominant uniaxial or biaxial loading, e.g. bone near a tendon insertion, orthogonal trabecular orientations that align with the loading direction minimize shear coupling. These observations suggest that optimal trabecular orientations near joint surfaces (like the proximal femur) may be different than those near tendon insertions (like the potoroo's calcaneus).

As discussed further below, these and other investigators draw an important distinction in functional environments that correlate with trabecular morphologies within traction apophyses (e.g. the trochanteric region and calcanei) *vs.* those that are within epiphyseal regions like the femoral neck (Heřt, 1992; Tsubota et al., 2002).

4.3. Tension/shear and cartilage: the cartilaginous growth plate is "protected"

Metaphyseal/epiphyseal trabecular architectural anisotropy, such as the arched patterns shown in the calcanei and femora in this study, might also be the circumstantial consequence of the disproportionate importance (Fig. 13) of minimizing the deleterious effects of tension and shear stress on cartilaginous growth plates (Inman, 1947; Moen

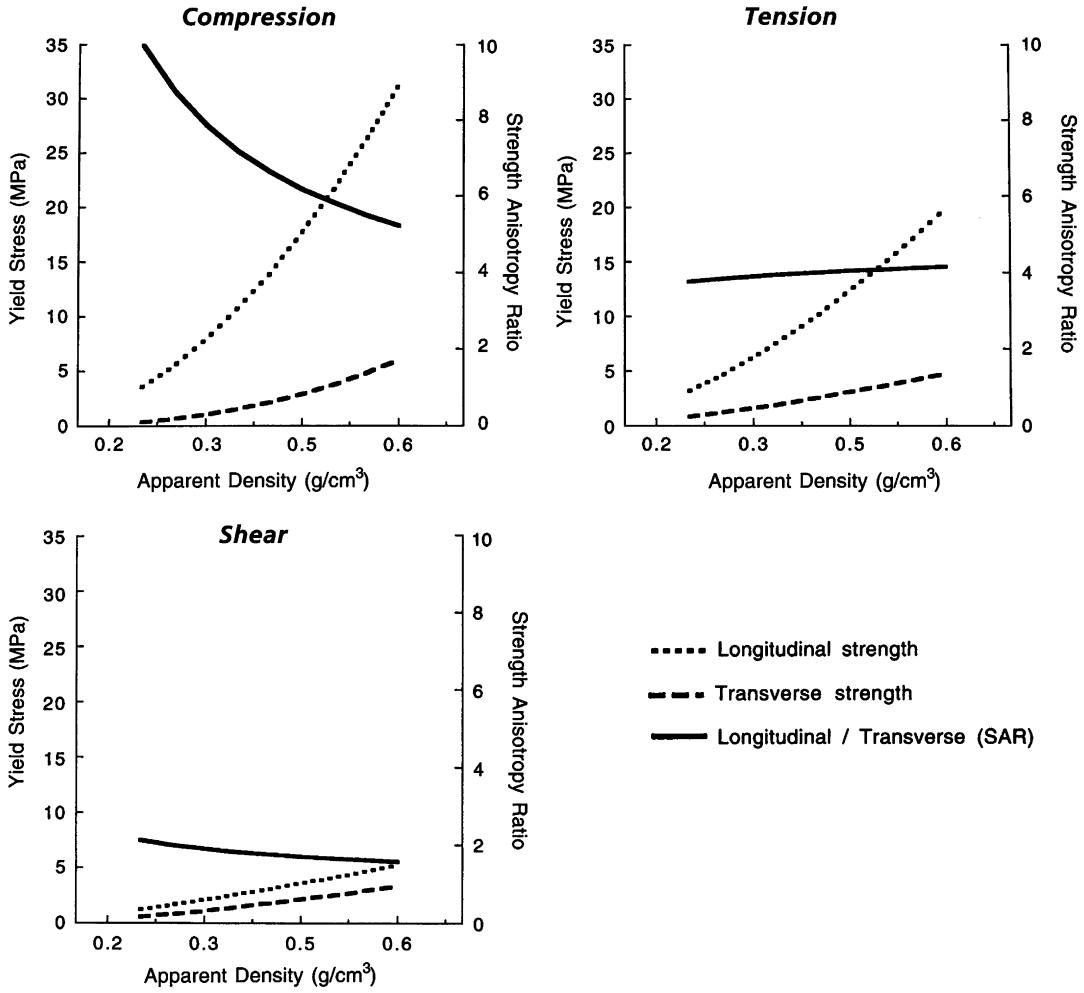

Fig. 14. Yield stress for longitudinal vs. transverse loading, and their ratio, plotted as a function of apparent density (i.e. bone volume fraction) for these different loading modes (compression, tension, and shear). The curves, based on data from bovine tibial trabecular bone (Keaveny et al., 1999), demonstrate the complexity of the strength properties of trabecular bone. Strength (dashed lines) always increases with increasing density and depends critically on loading direction and mode. The strength anisotropy ratio (**solid lines**) varies from approximately 2–10. It, too, depends on density and loading mode, being greatest for compression and *least for shear*. (Reproduced from Keaveny (2001) with permission of CRC press, Boca Raton, FL).

and Pelker, 1984; Smith, 1962a, b; Williams et al., 2001, 1999). This helps to avoid epiphyseal separation while enabling growth by avoiding excessive compression, consistent with the Hueter–Volkmann "law" (Mehlman et al., 1997; Moss-Salentijn, 1992). Biomechanical constraints on growth-plate orientation, in turn, could play an important role in governing the development of the trabecular patterns that subsequently form in these bones. Consequently, their trabecular patterns might be strongly, but less directly, correlated with mechanical stimuli—perhaps these stimuli *primarily* influence the cartilaginous growth plates that produce the trabeculae. If this interpretation is correct, then some trabecular patterns (e.g. see Swartz et al., 1998; Smith, 1962a) might not be as strongly associated with mechanical stimuli as conveyed by conventional wisdom. This supports shifting conventional emphasis from commonly ascribed, but nevertheless putative, roles for mechanobiological stimuli in the emergence of trabecular bone morphology (e.g. Carter and Beaupré, 2001; Tanck et al., 2006) to programmed pattern development that might more directly mediate the development of epiphyseal growth plates (Frost, 1990; Hamrick, 1999; Lovejoy, 2005).

But even this explanation is confounded by the fact that the 'weak' growth plate is progressively strengthened during ontogeny by formation of a stout perichondral ring (Chung et al., 1976), and the chance of epiphyseal separation is further reduced by greater tensile modulus than shear modulus of growth-plate cartilage (Cohen et al., 1992; Williams et al., 1999). Numerous observations suggest that a common characteristic of mammalian limb bones is that epiphyseal growth plates are generally oriented parallel to one of the principal stresses that occur in the region during normal activity (Smith, 1962a,b; Thompson, 1902). Consequently, in the human proximal femur and artiodactyl calcaneus the alignment of tensile

stress along their epiphyseal growth plates is a reasonable trade-off for avoiding the potentially more deleterious consequences if prevalent/predominant shear stresses were aligned along the growth plate.

Differing developmental 'fields' for trochanteric and neck regions. The biomechanical environments of the developing human and chimpanzee proximal femoral chondroepiphysis also significantly differ from artiodactyl calcanei since in these femora the apophyseal (greater trochanter) and epiphyseal (head) portions of the growth plate form in different developmental 'fields' (Kriz et al., 2002; Ogden, 1981, 1990; Reno et al., 2002; Siffert, 1983). During growth, the trochanteric and head regions progressively separate from what was previously a contiguous growth plate. The trochanteric region (mostly the greater trochanter) becomes a traction apophysis as a result of the loads that it receives from the gluteus medius. In contrast, the femoral head portion of the growth plate remains within the joint capsule and tends to become oriented orthogonal to the predominant compression loads across the hip joint (Smith, 1962a). The intervening cartilage (the 'interepiphyseal' region) gives rise to the arcuate (''tension'') trabecular tracts and the superior neck cortex of the subadult femur (Kriz et al., 2002; Ogden, 1981; Reno et al., 2002). These observations again demonstrate the inherent developmental/biomechanical complexities of the human proximal femur that render it an inadequate approximation of a natural trajectorial structure. Lovejoy (2004, p. 116) also emphasizes the possibility that, in contrast to the Wolffian paradigm, the arched trabecular pattern of the human proximal femur can be ''…readily explicable by interactive growth within its three physes—those of the head, greater trochanter, and the interepiphyseal ''band''.'' We speculate that trabeculae that form in traction apophyses more closely approximate strain-mode-related loading patterns whereas trabeculae that form in articular regions may be more strongly influenced by developmental constraints arising from patterning of the growth plate and articular surface geometries (Lovejoy et al., 2003). The idea that in some cases the developmental emergence of regional trabecular architectural anisotropy is not strongly influenced by mechanobiologic stimuli appears consistent with findings of Swartz et al. (1998) who were able to identify trabecular homologies across various species (mostly small mammals), suggesting a heritable program regulating the position of individual trabeculae.

4.4. Functional adaptation and pattern formation in the emergence of trabecular patterns: optimal, adequate, or circumstantial morphology?

Essentially, Wolff suggested that bone architecture was an answer to requirements of optimal stress transfer, pairing maximal strength to minimum weight, according to particular mathematical design rules (Huiskes, 2000). Huiskes (2000, pp. 153–154) states that even though sophisticated finite element models support Wolff's trajectorial hypothesis in continuous materials this:

> …in no way implies that bone cells actually use trajectorial information to form bone. As Cowin (1997) has pointed out again, this idea is sheer nonsense; any trabeculisation, any discontinuity in the material, would alter the stress trajectories, and the cells would forever chase their own tails trying to capture them in hard material. The correspondence between trabecular architecture and stress trajectories in models using continuous material representations is *circumstantial*, not causal.

This reflects the well-known fact that cortical and trabecular bone violate important assumptions of the trajectory hypothesis when applied in a strict/ideal context; namely, the material must be homogeneous, continuous, and isotropic (Brand et al., 2003; Cowin, 1989c; Harrigan et al., 1988; Heřt, 1992; Murray, 1936). In fact, as stated by Keaveny et al. (2001, p. 317), ''…the [mechanical] properties of trabecular bone are heterogeneous (vary with age, site, disease, etc), anisotropic (depend on loading direction), and asymmetric (differ in tension versus compression versus shear).'' Consequently, results of the present study showing that although all of the selected trabecular tracts in the calcanei and all of the stress trajectories in the simple beams are described by the equation $y^{-1} = a + b/x$, this equation probably does not have biophysical significance. Previous investigators have also suggested that such trabecular anisotropy may develop in a predetermined, minimally mechanically influenced fashion that circumstantially resembles stress/strain trajectories (Ascenzi and Bell, 1972; Huiskes, 2000; Jansen, 1920; Lovejoy, 2005; Lovejoy et al., 2002; Murray, 1936; Triepel, 1922). This appears to be supported by the fact that in developing deer and sheep calcanei the orientation of the epiphyseal growth plate and the plantar (''tension'') trabecular tracts are also described by the same nonlinear equation throughout ontogeny (from fetus to adult) (Skedros and Brady, 2001). But predictable patterns of dorsal-plantar stresses from muscle loading and other mechanobiologic stimuli probably exist and are likely present in utero, which might imply an important role for muscle loading in the emergence of this distinctive morphology (Carter and Beaupré, 2001; Skerry, 2000). For example, Skerry (2000) describes the unpublished qualitative observation of Lanyon and Goodship who, after transecting the Achilles tendon of a living fetal lamb, noted that subsequent prenatal growth produced disorganized trabeculae in the experimental calcaneus compared to the contralateral control. Although this isolated observation warrants confirmation, it suggests that prenatal loading might play an important role in the formation of the arched patterns described in the present study. Alternatively, the systematic expression of genetically derived positional information may be more directly important to a bone's development

than any individual effects of strain transduction. In this context, Lovejoy et al. (2002) state:

> Mounting evidence suggests that the role of mechanotransduction, especially in the developing/growing skeleton, is to provide necessary *threshold* values required for implementation or maintenance of patterns of growth guided principally by positional information, and it seems increasingly likely that this maxim holds as much for cancellous bone (i.e. trabecular distribution and orientation) as it does for cortex.

This view minimizes, or at least significantly reduces, the putative role that mechanical stimuli have in causally mediating the arched trabecular patterns in the human proximal femur and other bones. Additional studies examining this "developmental hypothesis" are warranted.

4.5. Impediments posed by the trajectory hypothesis and Wolff's "law

Recent scholars agree that the often vague or poor understanding of what Wolff's "law" actually is and the enormously variable ways that this nebulous rubric is used to explain normal and pathologic bone "transformation" processes (i.e. modeling and remodeling) are impediments to progress in understanding how mechanical stimuli and other biologic factors mediate normal skeletal development, maintenance, and adaptation (Bertram and Swartz, 1991; Cowin, 1997, 2001; Currey, 1997; Holt et al., 2004; Huiskes, 2000; Ruff et al., 2006). The historical acceptance of Wolff's "law" is partially rooted in orthopaedists' view that the human proximal femur and other bones and bone regions are subject to habitual 'tension/compression' stressing. This conception will be difficult to uproot, since, as noted by Hall (1985, p. xxv) "…specialists such as orthopaedic and oral surgeons and orthodontists spend their working lives manipulating the skeleton in conformity with the trajectory theory,…". This view reflects both: (1) the trajectorial hypothesis, and (2) a broader view (hence Hall's inclusion of "orthodontists") that Wolff's "law" includes consideration of putative trophic influences of tension and compression in bone development, adaptation, and fracture healing (Ascenzi and Bell, 1972; Lanyon, 1974; Pauwels, 1976; Zippel, 1992). This broader view actually more closely corresponds to Roux's view of "functional adaptation" in the skeleton and other organ systems (Dibbets, 1992; Lee and Taylor, 1999). The principal investigator of the present study is an orthopaedic surgeon who also recognizes this strong, if not dogmatic, influence in orthopaedic fracture fixation techniques, including applying metal plates on the "compression" surfaces of fractured long bones, reconstructing fractured bones with "tension-band" constructs, and implanting fixation screws or plates into the "compression" side of the femoral neck (Cheal et al., 1987; Schatzker, 1984; Tobin, 1955). Similar mechanical considerations are emphasized for conceptualizing stress transfer after the implantation of fracture fixation devices and intramedullary endoprostheses in the proximal femur (Finlay et al., 1991; Kyle, 1994; Lim et al., 1999; Meislin et al., 1990; Oh and Harris, 1978; Sim et al., 1995). Since the view of the proximal femur as a habitual 'tension/compression' region played a central role in the intellectual development and theoretical framework of Wolff's doctrine (see Appendix A), and because it continues to have an important influence in bone biomechanics and orthopaedic science, it must be more rigorously examined in controlled experimental conditions. This should include testing the hypothesis that age-related changes in the prevalence/predominance of bending loads across the proximal human femur explain regional decreases in trabecular bone mass (especially the 'tension' trabecular tracts) and cortical thickness (especially the 'tension' cortical region) that are associated with proximal femoral fragility fractures (Mayhew et al., 2005).

4.6. Weaknesses of the present study and future directions

There are several limitations inherent in the focus and methods of the present study. One of these is our use of plane roentgenograms, a second lies in our selection of obviously arched trabecular patterns, and a third is the use of closed-form mathematical descriptions of two-dimensional structures. These selection biases, although necessary for testing Wolff's hypothesis as historically founded on considerations of two-dimensional structures, does not allow for investigating other aspects of three-dimensional structural anisotropy and heterogeneity [e.g. trabecular length, thickness, and morphology (e.g. plates vs. rods), apparent density (i.e. volume fracture), and various measures of connectivity] that might reflect and/or affect resultant principal stresses. Although the arched trabecular patterns were readily discernable in the sectioned bones that we examined, three-dimensional measures of structural anisotropy could provide additional important biomechanical information (e.g. determining how variations in the degree of connectivity influence trabecular stress distribution). For example, in a study of high-resolution, materially nonlinear finite element models (used to obtain yield strains in both tension and compression) in 12 adult human femoral neck trabecular specimens, Bayraktar and Keaveny (2004) reported that "The highly oriented structure of trabecular bone results in equivalence of apparent-level yield and tissue-level strains for tensile loading but not from compression." This discrepancy was attributed to combined effects of the asymmetric strength of trabecular tissue (see Fig. 14) and the presence of slightly oblique trabeculae, causing tissue-level yield to occur first in tension for apparent compression loading. We suggest that this is a fundamental reason why three-dimensional morphologic differences would be expected between 'tension' and 'compression' trabecular regions, and especially in the intervening 'neutral axis' region or in regions generally subject to complex/multidirectional loading where shear stresses are prevalent/predominant. Addition-

ally, by carrying off-axis loads, some measures of trabecular connectivity and oblique cross struts can help reduce deleterious stress concentrations and shear deformations, and other nonlinear deformations such as bending and buckling that can be especially notable when trabecular volume fraction is low (e.g. with aging/osteoporosis) (Bayraktar and Keaveny, 2004; Ding et al., 2002; Parkinson and Fazzalari, 2003; Stauber et al., 2006; Van Rietbergen et al., 2003; Wang and Niebur, 2006). Some of these morphologic characteristics might evade recognition in the context of the traditional trajectorial paradigm. Micron-level imaging techniques coupled with computer modeling can allow for these more rigorous analyses of three-dimensional reconstructions (Bousson et al., 2004; Fajardo and Muller, 2001; Huiskes et al., 2000; Issever et al., 2003; Nuzzo et al., 2003; Odgaard, 2001; Van Rietbergen et al., 2003). Studies such as these are currently being conducted on the bones used in the present study.

A fourth limitation lies in our focus on Wolff's view of habitual loading of the hip. In this loading regime the angle of the joint contact force with respect to the femoral neck is relatively constant. There is evidence that the orientation of joint contact force is relatively consistent in many activities of daily living (Pedersen et al., 1997), and presumably, such habitual loading conditions drive bone adaptation. But less-frequent loading conditions may also produce strains or strain-related stimuli that are important in determining bone adaptation (Judex et al., 1997; Rubin et al., 2001; Rubin and McLeod, 1996; Turner et al., 1995). This contrasts with the idea that trabeculae tend to align with the *predominant* principal stress directions (both compressive and tensile), suggesting that higher magnitude stresses will have a disproportionately greater effect upon bone adaptation than smaller stresses (Biewener et al., 1996; Cheal et al., 1987; Frost, 1964, 1986; Hayes and Snyder, 1981; Lanyon, 1974; Lovejoy, 2005; Ryan and Ketcham, 2005b; Skerry and Lanyon, 1995; Turner, 1992).

5. Conclusion

Compared to the arched trabecular patterns in the cancellous bone of the human and chimpanzee femoral neck regions, the arched trabecular patterns in the sheep and deer calcanei more closely resemble stress trajectories in idealized, short, cantilevered beams. These beams also closely resemble Culmann's cantilevered beam—the historical 'origin' of Wolff's trajectorial hypothesis. The striking dichotomy between the arched trabecular patterns in these artiodactyl calcanei (orthogonal and symmetric) and these anthropoid femoral necks (nonorthogonal and asymmetric) might reflect differences in their developmental histories and habitual loading complexities. Biomechanical constraints associated with the orientation of cartilaginous growth plates, which may be disproportionately more important in cartilage than in cancellous bone, must also be considered because this directly influences the development of trabecular morphology. Furthermore, non-orthogonal patterns may reflect the relative "priority" that shear has over tension and compression (especially in trabecular bone) in causally mediating the emergence of developmental limb-bone adaptations. However, using quasi-parabolic trabecular patterns in these anthropoid bones to interpret loading history, and generalizing their utility for interpreting adaptation in other bones that are also not simply loaded, can be misleading because such architectural patterns can be variously influenced by diverse factors that often do not appear to have straightforward relationships with functional/mechanical stimuli. These results suggest that only some bones or bone regions subject to specific and relatively simple loading conditions (e.g. the calcanei) will exhibit what might be considered trajectorial patterns. Consequently, it is unfortunate that the relatively complexly loaded human femoral neck region has historically, and is often currently, modeled as a structure that generally conforms to Wolff's trajectorial paradigm. Further investigations are needed to determine the mechanisms that causally mediate functional adaptation of trabecular bone in the appendicular skeleton.

Acknowledgements

We thank Per Amundson and Jos Dibbets for translating portions of Julius Wolff's earlier works, Holgar Hennig for translating portions of Culmann's text, and Scott Sorenson, Mark Nielsen, Todd Pitts, Christian Sybrowsky, Kent Bachus, and Derinna Kopp for their criticisms on the manuscript. We are indebted to the librarians Mina Mandel and Brian Libbey for their help in obtaining the reference material, and to numerous libraries for the use of their collections, with most references being obtained from the University of Southern California Norris Medical Library, and the Louise M. Darling Biomedical Library at the University of California Los Angeles (UCLA). Per Amundson also spent several days in libraries in Germany obtaining reference material that we could not locate in the United States. We thank Kerry Matz for the original illustrations, Thomas Higgins for assuring the accuracy of stated implications for orthopaedic fixation devices, Roy Bloebaum for laboratory support, and Alan Goodship for providing the photograph of a Fairbairn crane. Chimpanzee bones were obtained from the Yerkes Primate Research Institute at Emory University, Atlanta, Georgia. This study was funded by medical research funds of the Department of Veteran's Affairs Medical Center, Salt Lake City, Utah, and The Utah Bone and Joint Center, Salt Lake City, Utah.

Appendix A

Wolff's "law": The concept of a causal form–function relationship expressed in cancellous architecture and causally mediated by dynamic loads that *seem* evident in bone growth is primarily the idea of Wolff's contemporary Wilhelm Roux (Dibbets, 1992; Fung, 1990; Huiskes, 2000;

Roesler, 1987). Contemporary application of Wolff's law of bone transformation can be summarized in three basic principles (Martin et al., 1998): (1) optimization of strength with respect to weight, (2) alignment of trabeculae with principal stress direction, and (3) self-regulation of bone structure by cells responding to a mechanical stimulus. Several authors provide further discussion of the origins, broad applications, common misconceptions, and notable inconsistencies of Wolff's "law" (Bertram and Swartz, 1991; Cowin, 2001; Currey, 1997; Dibbets, 1992; Lee and Taylor, 1999; Roesler, 1981; Treharne, 1981). Furthermore, as noted by Stanford and Brand (1999, p. 553), the use of "mathematical laws" in this context must be questioned since:

> Mathematical descriptions of natural phenomena never reflect causation, but rather merely describe and often accurately predict. Confusing description with causation has often led to the misunderstanding that mathematical "laws" "govern" or control or explain natural phenomena.

Bone "Transformation" vs. "Remodeling" vs. "Change in Conformation": During Wolff's time the concept of osteon-mediated remodeling was not known. Remodeling in this context is defined below. What Wolff referred to as "changes" or "transformation(s)" in bone architecture would actually be better translated as modeling (see below). It should also be noted that Wolff strongly ascribed to the concept of interstitial bone growth (Dibbets, 1992). The concept of modeling-mediated resorption vs. formation was debated in Wolff's time, but Wolff did not accept the somewhat limited evidence supporting the existence of modeling. Therefore, the processes of "remodeling", or "modeling" are not accurate translations of what Wolff referred to as "transformation" of bone. Wolff also considered his 'law' of bone transformation to apply to both cancellous and cortical bone, since cortical bone represented locations of high stress trajectory density, and these two tissues were basically the 'same', differing only in their porosities. Contemporary investigators have challenged this idea (Huiskes et al., 1987; Rice et al., 1988).

Modeling: Modeling activities affect the formation and/or resorption of secondary or non-secondary bone (e.g. primary bone, and trabecular bone in some cases) on periosteal or endosteal surfaces. They are detected as changes and/or differences in a bone's curvature, cross-sectional shape and/or regional cortical thickness. Consequently, modeling is a concept describing a combination of non-proximate, though coordinated, resorption and formation drifts whose net result is, typically, to change the distribution of bone (Jee et al., 1991). Such drifts are called macro-modeling in cortical bone and mini-modeling in cancellous bone (Frost, 1988a; Kobayashi et al., 2003). The re-alignment of trabecular tracts along the lines of stress would be a consequence of mini-modeling.

Remodeling: Remodeling activities affect the replacement of intracortical bone; this is achieved through the activation of basic multicellular units (BMUs = osteoclasts and osteoblasts) that create secondary osteons (Haversian systems) in cortical bone and secondary osteons or hemi-osteons in trabecular bone (Frost, 1986; Jee et al., 1991; Parfitt et al., 1996). During Wolff's time the concept of osteon-mediated remodeling was not known.

Wolff's "proof" that the human proximal femur is a natural trajectorial structure: The basic principles of Wolff's "law of bone transformation" were laid out in his papers published in 1869, 1870, 1872, and 1874. In 1869, Wolff argued that cancellous bone modeling adhered to mathematical rules, which he could prove corresponded to the principal stress trajectories in the Culmann 'crane'. As stated by Roesler (1981), Wolff's "proof" consisted of the following (Wolff, 1870, 1872):

(1) The irrefutable similarity between the two drawings recognizable "at the first sight" [compare Culmann's 'crane' and Wolff's femur in Figs. 3 and 6 of the present study],
(2) The crossing at right angles (orthogonal intersections) of the lines in the drawing of the cancellous bone structure he had made from frontal [coronal] sections of the human femur (Figs. 3 and 6),
(3) The corresponding crossing at right angles of the principal stress trajectories in the drawing of Culmann's 'crane',
(4) The construction of Culmann's 'crane' itself, the trajectories of which were obtained from the same load conditions as those of the human femur carrying the weight of the body.

As noted by Roesler (1981), these conditions may be necessary, but are not sufficient to prove Wolff's trajectory 'theory'. Therefore, it is more accurately referred to as the trajectory hypothesis.

On the origins of Culmann's 'crane' (Figs. 1, 3, and 6): Presumably under Culmann's supervision, one of his graduate students was primarily responsible for constructing the stress trajectories in this 'crane' in a manner (presumably) similar to that employed in drawing the stress trajectories in a Fairbairn crane (see "Fairbairn vignette" below) that Culmann had also illustrated in his textbook (Culmann, 1866; Rüttimann, 1992; Thompson, 1917, 1943) (Fig. 5A). Our examination of Culmann's text, however, suggests that different engineers may have determined the course of the curved trajectories in the Fairbairn crane and those in the Culmann 'crane'. Roesler states (1981, p. 35) that:

> No details about the construction of the famous crane [Culmann's 'crane'] have been handed down to us from Culmann himself …He [Wolff], however, claims that Culmann himself had gone over those parts of his publication which referred to the construction of the

> crane, and therefore they can be considered to be an authorized description. But it cannot be derived from Wolff's paper that Culmann also read the parts that contain Wolff's own deductions and conclusions from the drawing of the crane. Thus we must assume that Wolff made these deductions without the assistance of Culmann, who possibly could have helped to avoid at least the major misinterpretations of the trajectories of the crane.

Rüttimann quotes Rudolf Fick's recollection (italics) of the Culmann-Meyer meeting at the gathering of the Society for Natural Science in Zurich, July, 1866 with a correction of his own (non-italics):

> He (von Meyer) drew a crane similar to the shape of the upper end of the femur and asked …Culmann to draw in the tension and pressure lines to be calculated by him for this purpose, having already drawn trabeculae that were significant—in his opinion—on another piece of paper. Culmann had one of his pupils, Dr. Hedenauer, make the calculation and drawing and, just imagine, it corresponded with the one of H. Meyer….

The above-named assistant was not Dr. Hedenauer, but Dr. Andreas Rudolf Harlacher…

However, we have recognized that Culmann's associate (or student?) ''Bessard'' (only the eponym is noted in the text) supervised the illustration of a Fairbairn crane, which appears in Culmann's text (plate 11, Fig. 1) (Fig. 5A of the present study). This plate is referenced in Section 3, chapter 4 (pp. 264–270) of Culmann's text. The description of the mathematics for calculating stress trajectories appear in Section 2, chapter 4 (pp. 231–237). (Wolff (1870) primarily cites portions of Section 3, chapter 1 (pp. 209–226), which deals with mathematics and proofs related to calculating stress trajectories.) In contrast, Harlacher appears to have been responsible for plate 8 of Culmann's text, and for portions of Section 3, chapters 1 (pp. 219–223) and 2 (pp. 231–235); this section includes an illustration of the construction of the forces (Kräfte) within a rail resembling an I-beam. In this perspective it is plausible that there are different provenances of the stress trajectories of the Culmann 'crane' (Harlacher?) and Fairbairn crane (Bessard?). Additionally, the fact that the trajectories toward the free end of Culmann's 'crane' and the Fairbairn 'crane' are not superimposable (compare Figs. 1 and 5, Table 2) is consistent with our suggestion that different engineers (Culmann's ''students'') were involved in their creation. In turn, we speculate that the stress trajectories in the Fairbairn crane, being drawn at least 1 year before the publication of von Meyer's (1867) article (which includes the first published illustration of the Culmann 'crane' that we are aware of), were not constructed using methods identical to those used to draw the stress trajectories in the Culmann 'crane'.

Roesler's reconstruction of the Culmann 'crane'—the probable incorrect transition from beam to 'crane': The calcanei examined in the present study closely resemble the structures used in the initial formulation of the trajectorial paradigm—short, cantilevered beams loaded transversely at their free ends (Figs. 2, 4 and 7). Not only did Culmann's (1866) analyses on this topic originate from cantilevered beams, but the Culmann 'crane', popularized by Wolff, also appears to have a similar provenance (Roesler, 1981). In fact, Roesler (1981) suggests that the Culmann 'crane' was incorrectly constructed, citing two main engineering errors. Lee and Taylor (1999) summarize these as:

(1) Culmann's 'crane' was probably based on a straight cantilever having parabolic shearing stress distribution at its free end that, to make the geometry more consistent with the proximal femur, some curvature was added to this free end. However, no change was made to the stress distribution to allow for this curvature.
(2) To describe the state of stress in a curved bar with a parabolic or near-parabolic distribution of shearing stresses along its free end, three different stress components are required. Culmann's model involved only two components, a two-dimensional solution.

Roesler (1981) suggests that the creator of this 'crane' simply serially transected segments of a plane, straight cantilever, staggered them into the shape of a curve that approximated the shape of a Fairbairn crane, and added the missing trajectory segments, perhaps with a French curve. Hence, the Culmann 'crane' appears to be no more than a good first estimate of the stresses in the proximal femur. Wolff's mistake was to read more into analysis that was used to create the 'crane' than was technically justified. In this perspective, it is unfortunate that the trajectorial hypothesis has historically focused on the cancellous architecture of the comparatively complexly loaded human proximal femur.

Although Roesler's (Roesler, 1981) analysis seems generally plausible, there is evidence that the stress distribution *was modified* in both the Culmann 'crane' and the Fairbairn crane: Examination of these structures in Figs. 3 and 6 shows that the stress trajectories do not intersect on the neutral axis of the ''neck'' regions of either structure. In other words, it appears that a purposeful adjustment was made in the location of the neutral axis, which would be expected to be most obvious in the curvilinear portion of the beam (Mourtada et al., 1996). These structures nevertheless do not account for the loading complexity that is habitually experienced by the proximal femur, which was not well understood in Wolff's time.

Fairbairn vignette: Sir William Fairbairn (1789–1874) was a notable structural engineer who helped pioneer the use of iron in construction projects, especially bridges (Stephen and Lee, 1964). Since Fairbairn cranes (Fig. 5) are no longer in use, discussions about how they differed from other tower cranes can be found in encyclopaedias from the

late 1800s and early 1900s (e.g. The Encyclopaedia Britannica. 1910. Cranes, 11th Edition, Volume VII, pp. 368–372, Cambridge, England: at the University Press, New York, NY).

References

Aamodt, A., Lund-Larsen, J., Eine, J., Andersen, E., Benum, P., Schnell Husby, O., 1997. In vivo measurements show tensile axial strain in the proximal lateral aspect of the human femur. J Orthop Res 15, 927–931.

Akeson, W.H., Amiel, D., Kwan, M., Abitbol, J.J., Garfin, S.R., 1992. Stress dependence of synovial joints. In: Hall, B.K. (Ed.), Bone: Fracture Repair and Regeneration. CRC Press, Boca Raton, pp. 33–60.

Albert, E., 1900a. Die architectur der tibia. Wiener Med Wochenscrift (4, 5, & 6), 161–164, 219–224, 265–273.

Albert, E., 1900b. Einführung in das studium der architektur der röhrenknochen. Alfred Hölder. Vienna, Austria.

Alexander, R.M., 2004. Bipedal animals, and their differences from humans. J Anat 204, 321–330.

Arem, A.J., Madden, J.W., 1974. Is there a Wolff's law for connective tissue? Sur. Forum 25, 512–514.

Ascenzi, A., Bell, G.H., 1972. Bones as a mechanical engineering problem. In: Bourne, G.H. (Ed.), The Biochemistry and Physiology of Bone. Academic Press Inc., New York, pp. 311–352.

Backman, S., 1957. The proximal end of the femur: investigations with special reference to the etiology of femoral neck fractures; anatomical studies; roentgen projections; theoretical stress calculations; experimental production of fractures. Acta Radiol 146, 1–166.

Bacon, G.E., Bacon, P.J., Griffiths, R.K., 1984. A neutron diffraction study of the bones of the foot. J. Anat. 139, 265–273.

Bagi, C.M., Wilkie, D., Georgelos, K., Williams, D., Bertolini, D., 1997. Morphological and structural characteristics of the proximal femur in human and rat. Bone 21, 261–267.

Bähr, F., 1899. Beöbachtungen über die statischen Beziehungen des beckens zur uteren extremität. Deutsche. Ztschr. Orthop. Chir. 55, 52–59.

Barbieri, L., Buoncristiani, I., 1975. Considerations on some problems of osseous physiopathology in relation to a photoelastic study of the femur. Chir. Organ. Mov 62, 201–208.

Baumgaertner, M., Higgins, T., 2002. Femoral neck fractures. In: Bucholz, R., Heckman, J. (Eds.), Rockwood and Green's Fractures in Adults. Lippincott Williams and Wilkins, Philadelphia, PA, pp. 1579–1634.

Bay, B.K., Yerby, S.A., McLain, R.F., Toh, E., 1999. Measurement of strain distributions within vertebral body sections by texture correlation. Spine 24, 10–17.

Bayraktar, H.H., Keaveny, T.M., 2004. Mechanisms of uniformity of yield strains for trabecular bone. J. Biomech. 37, 1671–1678.

Beaupré, G.S., Orr, T.E., Carter, D.R., 1990. An approach for time-dependent bone modeling and remodeling-theoretical development. J. Orthop. Res. 8, 651–661.

Beck, T.J., Ruff, C.B., Warden, K.E., Scott, W.W., Gopala, U., 1990. Predicting femoral neck strength from bone mineral data: a structural approach. Invest. Radiol. 25, 6–18.

Bergmann, G., Graichen, F., Rohlmann, A., 1993. Hip joint loading during walking and running, measured in two patients. J. Biomech. 26, 969–990.

Bergmann, G., Deuretzbacher, G., Heller, M., Graichen, F., Rohlmann, A., Strauss, J., Duda, G.N., 2001. Hip contact forces and gait patterns from routine activities. J. Biomech. 34, 859–871.

Berquist, T.H., Coventry, M.B., 1992. The pelvis and hips. In: Berquist, T.H. (Ed.), Imaging of Orthopedic Trauma. W.B. Saunders Co, Philadelphia, PA, pp. 207–310.

Bertram, J.E., Swartz, S.M., 1991. The 'law of bone transformation': a case of crying Wolff? Biol. Rev. Camb. Philos. Soc. 66, 245–273.

Biewener, A.A., Swartz, S.M., Bertram, J.E.A., 1986. Bone modeling during growth: dynamic strain equilibrium in the chick tibiotarsus. Calcif Tissue Int. 39, 390–395.

Biewener, A.A., Fazzalari, N.L., Konieczynski, D.D., Baudinette, R.V., 1996. Adaptive changes in trabecular architecture in relation to functional strain patterns and disuse. Bone 19, 1–8.

Biewener, A.A., Thomason, J., Goodship, A., Lanyon, L.E., 1983. Bone stress in the horse forelimb during locomotion at different gaits: a comparison of two experimental methods. J. Biomech. 16, 565–576.

Black, M.D., 2004. Correspondence of trabecular and cortical geometries: a natural test of Wolff's Law. Am J Phys Anthrop. Suppl 38, 63.

Bloebaum, R.D., Lauritzen, R.S., Skedros, J.G., Smith, E.F., Thomas, K.A., Bennett, J.T., Hofmann, A.A., 1993. Roentgenographic procedure for selecting proximal femur allograft for use in revision arthroplasty. J. Arthroplasty. 8, 347–360.

Bousson, V., Peyrin, F., Bergot, C., Hausard, M., Sautet, A., Laredo, J.D., 2004. Cortical bone in the human femoral neck: three-dimensional appearance and porosity using synchrotron radiation. J. Bone Miner Res. 19, 794–801.

Bouvier, M., 1985. Application of in vivo bone strain measurement techniques to problems of skeletal adaptations. Yearbook of Physical Anthropology 28, 237–248.

Brand, R.A., Stanford, C.M., Swan, C.C., 2003. How do tissues respond and adapt to stresses around a prosthesis? A primer on finite element stress analysis for orthopaedic surgeons. Iowa Orthop. J. 23, 13–22.

Brickley-Parsons, D., Glimcher, M.J., 1984. Is the chemistry of collagen in intervertebral discs an expression of Wolff's Law? A study of the human lumbar spine. Spine 9, 148–163.

Bromage, T.G., Goldman, H.M., McFarlin, S.C., Warshaw, J., Boyde, A., Riggs, C.M., 2003. Circularly polarized light standards for investigations of collagen fiber orientation in bone. Anat. Rec. B. New Anat. 274, 157–168.

Brown, T.D., DiGioia, A.M., 1984. A contact-couples finite element analysis of the natural adult hip. J. Biomech. 17, 437–448.

Büdinger, K., 1903. Der spongiosabau der oberen extremität. Ztschr. Heilkunde XXIV, 1–82.

Bullough, P.G., Vigorita, V.J., 1984. Atlas of Orthopaedic Pathology with Clinical and Radiologic Correlations. J.B. Lippincott Co, Baltimore, MD.

Burger, E., Klein-Nulend, J., Smit, T., 2003. Strain-derived canalicular fluid flow regulates osteoclast activity in a remodelling osteon—a proposal. J. Biomech. 36, 1453–1459.

Carey, E.J., 1929. Studies in the dynamics of histogenesis. Radiology 13, 127–168.

Carter, D.R., Beaupré, G.S., 2001. Skeletal Function and Form. Cambridge University Press, Cambridge, UK, pp. 138–160.

Carter, D.R., Wong, M., 1988. Mechanical stresses and endochondral ossification in the chondroepiphysis. J. Orthop. Res. 6, 148–154.

Carter, D.R., Orr, T.E., Fyhrie, D.P., 1989. Relationships between loading history and femoral cancellous bone architecture. J. Biomech. 22, 231–244.

Chapman, M.W., Zickel, R.E., 1988. Subtrochanteric Fractures of the Femur. J. B. Lippincott Pub Co, New York, pp. 361–372.

Cheal, E.J., Hayes, W.C., Snyder, B.D., Nunamaker, D.M., 1987. Trabecular bone remodeling around smooth and porous implants in an equine patellar model. J. Biomech. 20, 1121–1134.

Chung, S.M., Batterman, S.C., Brighton, C.T., 1976. Shear strength of the human femoral capital epiphyseal plate. J. Bone Joint Surg. 58-A, 94–103.

Cohen, B., Chorney, G.S., Phillips, D.P., Dick, H.M., Buckwalter, J.A., Ratcliffe, A., Mow, V.C., 1992. The microstructural tensile properties and biochemical composition of the bovine distal femoral growth plate. J. Orthop. Res. 10, 263–275.

Cowin, S.C., 1984. Mechanical modeling of the stress adaptation process in bone. Calcif Tissue Int 36, S98–S103.

Cowin, S.C., 1986. Wolff's law of trabecular architecture at remodeling equilibrium. J. Biomech. Eng. 108, 83–88.

Cowin, S.C., 1989a. Mechanical properties of cancellous bone tissues. In: Cowin, S.C. (Ed.), Bone Mechanics. CRC Press, Boca Raton, FL, pp. 129–157.

Cowin, S.C., 1989b. A resolution restriction for Wolff's law of trabecular architecture. Bull. Hosp. Joint Dis. Orthop. Inst. 49, 205–212.

Cowin, S.C., 1989c. A resolution restriction for Wolff's law of trabecular architecture. Bull Hosp. Joint Dis. 49, 205–212.

Cowin, S.C., 1997. The false premise of Wolff's law. Forma 12, 247–262.

Cowin, S.C., 2001. The false premise in Wolff's law. In: Cowin, S.C. (Ed.), Bone Mechanics Handbook. CRC Press, Boca Raton, FL pp. 30-1–30-15.

Cristofolini, L., Viceconti, M., Cappello, A., Toni, A., 1996. Mechanical validation of whole bone composite femur models. J. Biomech. 29, 525–535.

Culmann, K., 1866. Die Graphische Statik. Verlag Von Meyer & Zeller, Zurich, Switzerland, p. 633.

Currey, J.D., 1984. The Mechanical Adaptations of Bone. Princeton University Press, Englewood Cliff, NJ, 294.

Currey, J.D., 1997. Was Wolff correct? Forma 12, 263–266.

D'Aout, K., Vereecke, E., Schoonaert, K., De Clercq, D., Van Elsacker, L., Aerts, P., 2004. Locomotion in bonobos (Pan paniscus): differences and similarities between bipedal and quadrupedal terrestrial walking, and a comparison with other locomotor modes. J. Anat. 204, 353–361.

Davy, D.T., Kotzar, G.M., Brown, R.H., Heiple, K.G., Goldberg, V.M., Heiple Jr., K.G., Berilla, J., Burstein, A.H., 1988. Telemetric force measurements across the hip after total arthroplasty. J. Bone Joint Surg. 70-A, 45–50.

Demes, B., Jungers, W.L., Walker, C., 2000. Cortical bone distribution in the femoral neck of strepsirhine primates. J. Hum. Evol. 39, 367–379.

Dibbets, J.M.H., 1992. One century of Wolff's law. In: Carlson, D.S., Goldstein, S.A. (Eds.), Bone Biodynamics in Orthodontic and Orthopedic Treatment. University of Michigan, Ann Arbor, MI, pp. 1–13.

Ding, M., Odgaard, A., Danielsen, C.C., Hvid, I., 2002. Mutual associations among microstructural, physical and mechanical properties of human cancellous bone. J. Bone Joint Surg. 84-B, 900–907.

Elftman, H., Manter, J., 1935. Chimpanzee and human feet in bipedal walking. Am. J. Phys. Anthrop. 20, 69–79.

Elke, R.P., Cheal, R.J., Simmons, C., Poss, R., 1995. Three-dimensional anatomy of the cancellous structures within the proximal femur from computed tomography data. J. Orthop. Res. 13, 513–523.

Fajardo, R.J., Muller, R., 2001. Three-dimensional analysis of nonhuman primate trabecular architecture using micro-computed tomography. Am. J. Phys. Anthropol. 115, 327–336.

Farkas, A., Milton, M.J., Hayner, J.C., 1948. An anatomical study of the mechanics, pathology, and healing of fracture of the femoral neck. J. Bone Joint Surg. 30-A, 53–69.

Fazzalari, N.L., Crisp, D.J., Vernon-Roberts, B., 1989. Mathematical modeling of trabecular bone structure: the evaluation of analytical and quantified surface to volume relationships in the femoral head and iliac crest. J. Biomech. 22, 901–910.

Fernandes, P., Rodrigues, H., Jacobs, C., 1999. A model of bone adaptation using a global optimisation criterion based on the trajectorial theory of Wolff. Comput. Methods Biomech. Biomed. Eng. 2, 125–138.

Field, R.E., Kenyon, C.M., 1989. A mathematical analysis for the modeling of trabecular bone. J. Biomed. Eng. 11, 384–389.

Finlay, J.B., Chess, D.G., Hardie, W.R., Rorabeck, C.H., Bourne, R.B., 1991. An evaluation of three loading configurations for the in vitro testing of femoral strains in total hip arthroplasty. J. Orthop. Res. 9, 749–759.

Ford, C.M., Keaveny, T.M., 1996. The dependence of shear failure properties of trabecular bone on apparent density and trabecular orientation. J. Biomech. 29, 1309–1317.

Forrester, J.C., Zederfeldt, B., Hayes, T.L., Hunt, T.K., 1970. Wolff's law in relation to the healing skin wound. J. Trauma 10, 770–779.

Fox, J.C., 2003. Biomechanics of the proximal femur: role of bone distribution and architecture. Mechanical Engineering, University of California at Berkeley. PhD Thesis, p. 151.

Francillon-Vieillot, H., de Buffrénil, V., Castanet, J., Géraudie, J., Meunier, F., Sire, J., Zylberberg, L., de Ricqlès, A., 1990. Microstructure and mineralization of vertebrate skeletal tissues. In: Carter, J. (Ed.), Skeletal Biomineralization: Patterns, Processes and Evolutionary Trends. Van Nostrand Reinhold, New York, pp. 471–530.

Frankel, V.H., 1960. The Femoral Neck: Function, Fracture Mechanisms, Internal Fixation: An Experimental Study. Charles C. Thomas, Springfield, IL, p. 120.

Freiberg, A.H., 1902. Wolff's law and the functional pathogenesis of deformity. Am. J. Med. Sci. 124, 956–972.

Frost, H.M., 1964. The Laws of Bone Structure. Thomas, Springfield, IL, p. 167.

Frost, H.M., 1986. Intermediary Organization of the Skeleton I and II. CRC Press Inc, Boca Raton, FL.

Frost, H.M., 1988a. Structural adaptations to mechanical usage. A proposed "three-way rule" for bone modeling. Part I. Vet. Compar. Orthop. Traumatol. 1, 7–17.

Frost, H.M., 1988b. Structural adaptations to mechanical usage. A proposed "three-way rule" for bone modeling. Part II. Vet. Compar. Orthop. Traumatol. 2, 80–85.

Frost, H.M., 1990. Skeletal structural adaptations to mechanical usage (SATMU): 3. The hyaline cartilage modeling problem. Anat. Rec. 226, 423–432.

Fung, Y.C., 1990. Biomechanical Aspects of Growth and Tissue Engineering. Springer, New York, pp. 499–546.

Ganey, T.M., Ogden, J.A., 1998. Pre- and post-natal development of the hip. In: Callaghan, J.J., Rosenbery, A.G., Rubash, H.E. (Eds.), The Adult Hip. Lippincott-Raven Publishers, Philadelphia, PA, pp. 39–55.

Garden, R.S., 1961. The structure and function of the proximal end of the femur. J. Bone Joint Surg. 43-B, 576–589.

Gibson, L.J., Ashby, M.F., 1997. Cancellous bone. In: Ward, I.M. (Ed.), Cellular Solids: Structure and Properties. Cambridge University Press, Cambridge, UK, pp. 429–452.

Greenspan, A., 1988. Orthopaedic Radiology: A Practical Approach. JB Lippincott, Philadelphia, PA, pp. 5.19–5.20.

Greenspan, S.L., Myers, E.R., Kiel, D.P., Parker, R.A., Hayes, W.C., Resnick, N.M., 1998. Fall direction, bone mineral density, and function: risk factors for hip fracture in frail nursing home elderly. Am. J. Med. 104, 539–545.

Hall, B.K., 1985. Introduction. In: Murray, P.D.F. (Ed.), Bones. Cambridge University Press, New York, pp. xi–xxxii.

Hamrick, M.W., 1999. A chondral modeling theory revisited. J. Theor. Biol. 201, 201–208.

Harrigan, T.P., Jasty, M., Mann, R.W., Harris, W.H., 1988. Limitations of the continuum assumption in cancellous bone. J. Biomech. 21, 269–275.

Harty, M., 1984. The Anatomy of the Hip Joint. Springer, New York, NY, pp. 45–74.

Hayes, W.C., Snyder, B., 1981. Toward a quantitative formulation of Wolff's law in trabecular bone. In: Cowin, S.C. (Ed.), Mechanical Properties of Bone. The American Society of Mechanical Engineers, New York, pp. 43–68.

Herrera, M., Panchon, A., Perez-Bacete, M., 2001. Trabecular trajectory in the articular process of the human fourth cervical vertebrae. J. Anat. 199, 345–348.

Heřt, J., 1992. A new explanation of the cancellous bone architecture. Funct. Dev. Morphol. 2, 17–24.

Heřt, J., 1994. A new attempt at the interpretation of the functional architecture of the cancellous bone. J. Biomech. 27, 239–242.

Heřt, J., Fiala, P., Jirova, J., 2001. Mechanical loading of the human femoral neck. Acta. Chir. Orthop. Traumatol. Cech. 68, 222–229.

Hodge, W.A., Fijan, R.S., Carlson, K.L., Burgess, R.G., Harris, W.H., Mann, R.W., 1986. Contact pressures in the human hip joint measured in vivo. Proc. Natl. Acad. Sci. USA 83, 2879–2883.

Holt, B.M., Ruff, C.B., Trinkaus, E., 2004. The Wolff's law debate: throwing water out, but keeping the baby. Am. J. Phys. Anthrop. Suppl. 38, 115–116.

Huiskes, R., 2000. If bone is the answer, then what is the question? J. Anat. 197, 145–156.

Huiskes, R., Janssen, J.D., Slooff, T.J., 1981. A detailed comparison of experimental and theoretical stress-analyses of a human femur. In: Cowin, S.C. (Ed.), Mechanical Properties of Bone. The American Society of Mechanical Engineers, New York, pp. 211–234.

Huiskes, R., Weinans, H., Grootenboer, H.J., Dalstra, M., Fudala, B., Slooff, T.J., 1987. Adaptive bone-remodeling theory applied to prosthetic-design analysis. J. Biomech. 20, 1135–1150.

Huiskes, R., Ruimerman, R., van Lenthe, G.H., Janssen, J.D., 2000. Effects of mechanical forces on maintenance and adaptation of form in trabecular bone. Nature 405, 704–706.

Inman, V., 1947. Functional aspects of the abductor muscles of the hip. J. Bone Joint Surg. 29-A, 607–619.

Issever, A.S., Walsh, A., Lu, Y., Burghardt, A., Lotz, J.C., Majumdar, S., 2003. Micro-computed tomography evaluation of trabecular bone structure on loaded mice tail vertebrae. Spine 28, 123–128.

Jacobs, C.R., Simo, J.C., Beaupre, G.S., Carter, D.H., 1997. Adaptive bone remodeling incorporating simultaneous density and anisotropy considerations. J. Biomech. 30, 603–613.

Jansen, M., 1920. On Bone Formation: Its Relation to Tension and Pressure. Manchester University Press, Longmans, Green and Co, London, UK, p. 114.

Jee, W.S.S., Li, X.J., Ke, H.Z., 1991. The skeletal adaptation to mechanical usage in the rat. Cells Mater. 1, 131–142.

Jenkins Jr., F.A., 1972. Chimpanzee bipedalism: cineradiographic analysis and implications for the evolution of gait. Science 178, 877–879.

Joshi, M.G., Advani, S.G., Miller, F., Santare, M.H., 2000. Analysis of a femoral hip prosthesis designed to reduce stress shielding. J. Biomech. 33, 1655–1662.

Judex, S., Gross, T.S., Bray, R.C., Zernicke, R.F., 1997. Adaptation of bone to physiological stimuli. J. Biomech. 30, 421–429.

Kachigan, S.K., 1986. Statistical Analysis. Radius Press, New York, NY, p. 589.

Kalmey, J.K., Lovejoy, C.O., 2002. Collagen fiber orientation in the femoral necks of apes and humans: do their histological structures reflect differences in locomotor loading? Bone 31, 327–332.

Kapandji, I., 1987. The Physiology of Joints: Lower Limb 2. Churchill Livingstone, Edinburgh, UK, p. 219.

Kawashima, T., Uhthoff, H.K., 1991. Pattern of bone loss of the proximal femur: a radiologic, densitometric, and histomorphometric study. J. Orthop. Res. 9, 634–640.

Keaveny, T.M., 2001. Strength of trabecular bone. In: Cowin, S.C. (Ed.), Bone Mechanics Handbook. CRC Press, Boca Raton, FL pp. 16-1–16-42.

Keaveny, T.M., Hayes, W.C., 1993. Mechanical properties of cortical and trabecular bone. In: Hall, B.K. (Ed.), Bone. CRC Press, Boca Raton, FL, pp. 285–344.

Keaveny, T.M., Wachtel, E.F., Cutler, M.J., Pinilla, T.P., 1994. Yield strains for bovine trabecular bone are isotropic but asymmetric. Trans. Orthop. Res. Soc. 19, 428.

Keaveny, T.M., Wachtel, E.F., Zadesky, S.P., Arramon, Y.P., 1999. Application of the Tsai-Wu quadratic multiaxial failure criterion to bovine trabecular bone. J. Biomech. Eng. 121, 99–107.

Keaveny, T.M., Morgan, E.F., Niebur, G.L., Yeh, O.C., 2001. Biomechanics of trabecular bone. Annu. Rev. Biomed. Eng. 3, 307–333.

Keith, A., 1919. Menders of the Maimed: The Anatomical and Physiological Principles Underlying the Treatment of Injuries to Muscles, Nerves, Bones, and Joints. J.B. Lippincott Company, Philadelphia, PA, p. 335.

Kennedy, K.A.R., 1989. Skeletal markers of occupational stress. In: İşcan, M.Y., Kennedy, K.A.R. (Eds.), Reconstruction of Life from the Skeleton. Alan R. Liss, Inc, New York, pp. 129–160.

Kerr, W.C., Bishop, A.R., 1986. Dynamics of structural phase transitions in highly anisotropic systems. Phys. Rev. B. Condens. Matter 34, 6295–6314.

Kerr, R., Resnick, D., Sartoris, D.J., Kursunoglu, S., Pineda, C., Haghighi, P., Greenway, G., Guerra Jr., J., 1986. Computerized tomography of proximal femoral trabecular patterns. J. Orthop. Res. 4, 45–56.

Knothe Tate, M.L., 2003. "Whither flows the fluid in bone?" An osteocyte's perspective. J. Biomech. 36, 1409–1424.

Kobayashi, S., Takahashi, H.E., Ito, A., Saito, N., Nawata, M., Horiuchi, H., Ohta, H., Iorio, R., Yamamoto, N., Takaoka, K., 2003. Trabecular minimodeling in human iliac bone. Bone 32, 163–169.

Koch, J.C., 1917. The laws of bone architecture. Am. J. Anat. 21, 177–298.

Kothari, M., Keaveny, T.M., Lin, J.C., Newitt, D.C., Genant, H.K., Majumdar, S., 1998. Impact of spatial resolution on the prediction of trabecular architecture parameters. Bone 22, 437–443.

Koval, K.J., Zuckerman, J.D., 2002. Handbook of Fractures. Lippincott Williams & Wilkins, Philadelphia, PA, p. 466.

Kriz, M.A., 2002. The surface anatomy, internal structure, and external morphology of the mammalian proximal femur with special reference to its developmental biology. Anthropology, Kent State, Kent Ohio. Masters of Arts, 89.

Kriz, M.A., Reno, P.L., Lovejoy, C.O., 2002. Morphometric variation in proximal femoral development in primates and mammals. Am. J. Phys. Anthrop. Suppl 34, 97.

Kumaresan, S., Yoganandan, N., Pintar, F.A., Maiman, D.J., Goel, V.K., 2001. Contribution of disc degeneration to osteophyte formation in the cervical spine: a biomechanical investigation. J. Orthop. Res. 19, 977–984.

Kummer, B., 1959. Bauprinzipien des Säugerskeletes Georg Thieme Verlag. Stuttgart, Germany, p. 235.

Kuo, T., Skedros, J.G., Bloebaum, R.D., 1998. Comparison of human, primate and canine femora: Implications for biomaterials testing in total hip replacement. J. Biomed. Mater Res. 40, 475–489.

Kuo, T., Skedros, J.G., Bloebaum, R.D., 2003. Measurement of the femoral anteversion by biplane radiography and ct imaging; comparison with an anatomic reference. Invest. Radiol. 38, 221–229.

Kyle, R., 1994. Fractures of the proximal part of the femur. J. Bone Joint Surg. 76-A, 924–951.

Lanyon, L.D., 1973. Analysis of surface bone strain in the calcaneus of sheep during normal locomotion. J. Biomech. 6, 41–49.

Lanyon, L.E., 1974. Experimental support for the trajectorial theory of bone structure. J. Bone Joint Surg. 56-B, 160–166.

Lanyon, L.E., Rubin, C.T., 1985. Functional adaptation in skeletal structures. In: Hildebrand, M., Bramble, D.M., Liem, K.F., Wake, D.B. (Eds.), Functional Vertebrate Morphology. The Belkap Press of Harvard University Press, Cambridge, MA, pp. 1–25.

Laroche, M., Ludot, I., Thiechart, M., Arlet, J., Pieraggi, M., Chiron, P., Moulinier, L., Cantagrel, A., Puget, J., Utheza, G., Mazieres, B., 1995. Study of the interosseous vessels of the femoral head in patients with fractures of the femoral neck or osteoarthritis of the hip. Osteop. Int. 5, 213–217.

Laros, G., 1990. Intertrochanteric fractures. In: McCollister, E. (Ed.), Surgery of the Musculoskeletal System. Churchill Livingstone, New York, pp. 2613–2639.

Lee, T.C., Taylor, D., 1999. Bone remodeling: should we cry Wolff? Ir. J. Med. Sc. 168, 102–105.

Lim, L.-A., Carmichael, S.W., Cabanela, M.E., 1999. Biomechanics of total hip arthroplasty. Anat. Rec. 257, 110–116.

Löer, F., Weigmann, R., 1992. Julius Wolff and Friedrich Pauwels: Wolff's concept of a causal therapy of orthopaedic diseases using biological adaptation phenomena and its realization by Friedrich Pauwels. In: Regling, G. (Ed.), Wolff's Law and Connective Tissue Regulation. Walter de Gruyter, New York, pp. 23–30.

Lotz, J.C., Cheal, E.J., Hayes, W.C., 1995. Stress distributions within the proximal femur during gait and falls: implications for osteoporotic fracture. Osteop. Int. 5, 252–261.

Lovejoy, C.O., 2005. The natural history of human gait and posture. Part 2. Hip and thigh. Gait Posture 21, 113–124.

Lovejoy, C.O., Heiple, K.G., Meindl, R.S., Ohman, J.C., White, T.D., 2002. The Maka femur and its bearing on the antiquity of human walking: applying contemporary concepts of morphogenesis to the human fossil record. Am. J. Phys. Anthropol. 119, 97–133.

Lovejoy, C.O., McCollum, M.A., Reno, P.L., Rosenman, B.A., 2003. Developmental biology and human evolution. Annu. Rev. Anthropol. 32, 85–109.

Macchiarelli, R., Bondioli, L., Galichon, V., Tobias, P., 1999. Hip bone trabecular architecture shows uniquely distinctive locomotor behaviour in South African australopithecines. J. Hum. Evol. 36, 211–232.

Maquet, P.J., 1985. Biomechanics of the Hip: As Applied to Osteoarthritis and Related Conditions. Springer, New York, p. 309.

Markolf, K.L., 1991. Biomechanics of the hip. In: Amstutz, H.C. (Ed.), Hip Arthroplasty. Churchill Livingstone, New York, pp. 15–23.

Martin, R.B., Burr, D.B., Sharkey, N.A., 1998. Skeletal Tissue Mechanics. Springer, New York, p. 392.

Martini, F.H., 1995. Fundamentals of Anatomy and Physiology. Prentice Hall, Upper Saddle River, NJ, p. 1144.

Martinón-Torres, M., 2003. Quantifying trabecular orientation in the pelvic cancellous bone of modern humans, chimpanzees, and the Kebara 2 Neanderthal. Am. J. Hum. Biol. 15, 647–661.

Mason, M.W., Skedros, J.G., Bloebaum, R.D., 1995. Evidence of strain-mode-related cortical adaptation in the diaphysis of the horse radius. Bone 17, 229–237.

Mayhew, P.M., Thomas, C.D., Clement, J.G., Loveridge, N., Beck, T.J., Bonfield, W., Burgoyne, C.J., Reeve, J., 2005. Relation between age, femoral neck cortical stability, and hip fracture risk. Lancet 366, 129–135.

McHenry, H.M., 1975. The ischium and hip extensor mechanism in human evolution. Am. J. Phys. Anthropol. 43, 39–46.

Mehlman, C.T., Araghi, A., Roy, D.R., 1997. Hyphenated history: the Hueter–Volkmann law. Am. J. Orthop. 26, 798–800.

Meislin, R.J., Zuckerman, J.D., Kummer, F.J., Frankel, V.H., 1990. A biomechanical analysis of the sliding hip screw: the question of plate angle. J. Orthop. Trauma. 4, 106–130.

Miller, M.D., 1996. Review of Orthopaedics. W.B. Saunders Company, Philadelphia, PA, p. 510.

Miller, Z., Fuchs, M.B., Arcan, M., 2002. Trabecular bone adaptation with an orthotropic material model. J. Biomech. 35, 247–256.

Moen, C.T., Pelker, R.R., 1984. Biomechanical and histological correlations in growth plate failure. J. Pediatr. Orthop. 4, 180–184.

Moore, K.L., 1985. Clinically Oriented Anatomy. Williams and Wilkins, Baltimore, MD, p. 1101.

Morris, J.M., 1971. Biomechanical aspects of the hip joint. Orthop. Clin. North Am. 2, 33–54.

Möser, M., Hein, W., 1987. Krafte an der hufte—das Unteergurtmodell. Beitr Orthop Traumatol 34, 83–92, 179-189.

Moss-Salentijn, L., 1992. Long bone growth. In: Hall, B.K. (Ed.), Bone. CRC Press, Boca Raton, FL, p. 6 Bone growth—A, pp. 185–208.

Mourtada, F.A., Beck, T.J., Hauser, D.L., Ruff, C.B., Bao, G., 1996. Curved beam model of the proximal femur for estimating stress using dual-energy X-ray absorptiometry derived structural geometry. J. Orthop. Res. 14, 483–492.

Murray, P.D.F., 1936. Bones: A Study of the Development and Structure of the Vertebrate Skeleton. Cambridge University Press, Cambridge, UK, p. 203.

Myers, E.R., Wilson, S.E., 1997. Biomechanics of osteoporosis and vertebral fracture. Spine 22, 25S–31S.

Neville, A.C., 1993. Biology of Fibrous Composites: Development Beyond the Cell Membrane. Cambridge University Press, New York, p. 214.

Nuzzo, S., Meneghini, C., Braillon, P., Bouvier, R., Mobilio, S., Peyrin, F., 2003. Microarchitectural and physical changes during fetal growth in human vertebral bone. J. Bone Miner Res. 18, 760–768.

Oatis, C., 2004. Structure and function of the bones and noncontractile elements of the hip. In: Kinesiology: The Mechanics and Pathomechanics of Human Movement. Lippincott Williams and Wilkins, Philadelphia, PA, pp. 663–678.

Odgaard, A., 2001. Quantification of cancellous bone architecture. In: Cowin, S.C. (Ed.), Bone Mechanics Handbook. CRC Press, Boca Raton, FL pp. 14-1–14-19.

Ogden, J.A., 1981. Hip development and vascularity: relationship to chondro-osseous trauma in the growing child. In: Ogden, J.A. (Ed.), The Hip. CV Mosby, St. Louis, Mo.

Ogden, J.A., 1990. Femur. In: Ogden, J.A. (Ed.), Skeletal Injury in the Child. W.B. Saunders Co., Philadelphia, PA, pp. 683–744.

Oh, I., Harris, W.H., 1978. Proximal strain distribution in the loaded femur. An in vitro comparison of the distributions in the intact femur and after insertion of different hip-replacement femoral components. J. Bone Joint Surg. 60-A, 75–85.

Osborne, D., Effmann, E., Broda, K., Harrelson, J., 1980. The development of the upper end of the femur, with special reference to its internal architecture. Radiology 137, 71–76.

Oxnard, C.E., Yang, H.C.L., 1981. Beyond biometrics: studies of complex biological patterns. In: Ashton, E.H., Holmes, R.L. (Eds.), Perspectives in Primate Biology (The Proceedings of a Symposium Held at the Zoological Society of London 31 May and 1 June 1979). Academic Press, London, UK, pp. 127–167.

Parfitt, A.M., Mundy, G.R., Roodman, G.D., Hughes, D.E., Boyce, B.F., 1996. A new model for the regulation of bone resorption, with particular reference to the effects of bisphosphonates. J. Bone Miner Res. 11, 150–159.

Parkinson, I.H., Fazzalari, N.L., 2003. Interrelationships between structural parameters of cancellous bone reveal accelerated structural change at low bone volume. J. Bone Miner Res. 18, 2200–2205.

Pauwels, F., 1976. Biomechanics of the Normal and Diseased Hip: Theoretical Foundation, Technique, and Results of Treatment. Springer, New York, p. 276.

Pedersen, D.R., Brand, R.A., Davy, D.T., 1997. Pelvic muscle and acetabular contact forces during gait. J. Biomech. 30, 959–965.

Phillips, J.R., Williams, J.F., Melick, R.A., 1975. Prediction of the strength of the neck of femur from its radiological appearance. Biomed. Eng. 10, 367–372.

Pidaparti, R.M.V., Turner, C.H., 1997. Cancellous bone architecture: advantages of nonorthogonal trabecular alignment under multidirectional loading. J. Biomech. 30, 979–983.

Pinilla, T.P., Boardman, K.C., Bouxsein, M.L., Myers, E.R., Hayes, W.C., 1996. Impact direction from a fall influences the failure load of the proximal femur as much as age-related bone loss. Calcif. Tissue Int. 58, 231–235.

Pontzer, H., Lieberman, D.E., Momin, E., Devlin, M.J., Polk, J.D., Hallgrimsson, B., Cooper, D.M., 2006. Trabecular bone in the bird knee responds with high sensitivity to changes in load orientation. J. Exp. Biol. 209, 57–65.

Radin, E.L., Blaha, J.D., Rose, R.M., Litsky, A.A., 1992. Practical Biomechanics for the Orthopaedic Surgeon. Churchill Livingstone, New York, p. 216.

Rasch, P.J., Burke, R.K., 1978. Kinesiology and Applied Anatomy. Lea & Febiger, Philadelphia, PA, p. 496.

Reddy, M.S., Geurs, N.C., Wang, I.C., Liu, P.R., Hsu, Y.T., Jeffcoat, R.L., Jeffcoat, M.K., 2002. Mandibular growth following implant restoration: does Wolff's law apply to residual ridge resorption? Int. J. Periodont. Restor. Dent. 22, 315–321.

Reno, P.L., Kriz, M.A., McCollum, M.A., Lovejoy, C.O., 2002. Scanning electron microscopic analysis of regional histomorphological variations within the physis of the primate proximal femur. Am. J. Phys. Anthrop. Suppl 34, 130.

Resnick, D., Niwayama, G., 1988. Osteoporosis. In: Resnick, D., Niwayama, G. (Eds.), Diagnosis of Bone and Joint Disorders. WB Saunders Co, Philadelphia, PA, pp. 2022–2085.

Rice, J.C., Cowin, S.C., Bowman, J.A., 1988. On the dependence of the elasticity and strength of cancellous bone on apparent density. J. Biomech. 21, 155–168.

Richmond, B.G., Nakatsukasa, R., Ketcham, R., Hirakawa, T., 2004. Trabecular bone structure in human and chimpanzee knee joints. Am. J. Phys. Anthrop. Suppl 38, 167.

Roesler, H., 1981. Some historical remarks of the theory of cancellous bone structure (Wolff's Law). In: Cowin, S.C. (Ed.), Mechanical Properties of Bone. The American Society of Mechanical Engineers, New York, pp. 27–42.

Roesler, H., 1987. The history of some fundamental concepts in bone biomechanics. J. Biomech. 20, 1025–1034.

Rook, L., Bondioli, L., Kohler, M., Moya-Sola, S., Macchiarelli, R., 1999. Oreopithecus was a bipedal ape after all: evidence from the iliac cancellous architecture. Proc. Natl. Acad. Sci. USA. 96, 8795–8799.

Rosenthal, D.I., Scott, J.A., 1983. Biomechanics important to interpret radiographs of the hip. Skel. Radiol. 9, 185–188.

Rubin, C.T., 1988. Response of bone to mechanical stimulation. In: Dee, R. (Ed.), Principles of Orthopaedic Practice. McGraw-Hill Book Company, New York, pp. 79–89.

Rubin, C.T., Hausman, M.R., 1988. The cellular basis of Wolff's law. Transduction of physical stimuli to skeletal adaptation. Rheum. Dis. Clin. North Am. 14, 503–517.

Rubin, C.T., McLeod, K.J., 1996. Inhibition of osteopenia by biophysical intervention. In: Marcus, R., Feldman, D., Kelsey, J. (Eds.), Osteoporosis. Academic Press, New York, pp. 351–371.

Rubin, C., Gross, T., Qin, Y.X., Fritton, S., Guilak, F., McLeod, K., 1996. Differentiation of the bone-tissue remodeling response to axial and torsional loading in the turkey ulna. J. Bone Joint Surg. 78-A, 1523–1533.

Rubin, C., Turner, A.S., Bain, S., Mallinckrodt, C., McLeod, K., 2001. Low mechanical signals strengthen long bones. Nature 412, 603–604.

Ruff, C.B., Hayes, W.C., 1983. Cross-sectional geometry of Pecos Pueblo femora and tibiae-A biomechanical investigation: 1. Method and general patterns of variation. Am. J. Phys. Anthrop. 60, 359–381.

Ruff, C.B., Hayes, W.C., 1984. Bone-mineral content in lower limb. Relationship to cross-sectional geometry. J. Bone Joint Surg. 66-A, 1024–1031.

Ruff, C., Holt, B., Trinkaus, E., 2006. Who's afraid of the big bad Wolff?: "Wolff's law" and bone functional adaptation. Am. J. Phys. Anthropol. 129, 484–498.

Rüttimann, B., 1992. A noteworthy meeting of the society for nature research in Zurich: Two important precursors of Julius Wolff: Carl Culmann and Hermann von Meyer. In: Regling, G. (Ed.), Wolff's Law and Connective Tissue Regulation. Walter de Gruyter, New York, pp. 13–22.

Ryan, T.M., Ketcham, R.A., 2005a. Angular orientation of trabecular bone in the femoral head and its relationships to hip joint loads in leaping primates. J. Morphol. 265, 249–263.

Ryan, T.M., Ketcham, R.A., 2005b. Angular orientation of trabecular bone in the femoral head and its relationships to hip joint loads in leaping primates. J. Morphol. 265, 249–263.

Rydell, N.W., 1966. Forces acting on the femoral head-prosthesis. A study on strain gauge supplied prostheses in living persons. Acta Orthop. Scand. 37 (Suppl 88), 1–132.

Sabry, F.F., Ebraheim, N.A., Rezcallah, A.T., 2000. Internal architecture of the calcaneus: implications for calcaneus fractures. Foot Ankle Int 21, 114–118.

Schatzker, J., 1984. Subtrochanteric fractures of the femur. In: The Rationale of Operative Fracture Care. Springer, Berlin, Germany, pp. 217–234.

Schatzker, J., 1991. Screws and plates and their application. In: Müller, M.E., Allgöwer, M., Schneider, R., Willenegger, H. (Eds.), Manual of Internal Fixation-Techniques Recommended by the AO-ASIF Group. Springer, New York, pp. 179–290.

Schmitt, D., 2003. Insights into the evolution of human bipedalism from experimental studies of humans and other primates. J. Exp. Biol. 206, 1437–1448.

Siffert, R.S., 1983. Patterns of deformity of the developing hip. In: Katz, J.F., Siffert, R.S. (Eds.), Management of Hip Disorders in Children. J.B. Lippincott Co, Philadelphia, PA, pp. 73–91.

Sim, E., Freimuller, W., Reiter, T.J., 1995. Finite element analysis of the stress distributions in the proximal end of the femur after stabilization of a pertrochanteric model fracture: a comparison of two implants. Injury 26, 445–449.

Sinclair, D., Dangerfield, P., 1998. Human Growth After Birth. Oxford University Press, New York, p. 71.

Singh, M., Nagrath, A.R., Maini, P.S., 1970. Changes in trabecular pattern of the upper end of the femur as an index of osteoporosis. J. Bone Joint Surg. 52-A, 457–467.

Skedros, J.G., 2001. Collagen fiber orientation: a characteristic of strain-mode-related regional adaptation in cortical bone. Bone 28, S110–S111.

Skedros, J.G., Bloebaum, R.D., 1991. Geometric analysis of a tension/compression system: implications for femoral neck modeling. Trans. Orthop. Res. Soc. 37th Annual Meeting, 421.

Skedros, J.G., Brady, J.H., 2001. Ontogeny of cancellous bone anisotropy in a natural "trajectorial structure": genetics or epigenetics. J. Bone Miner. Res. Suppl. 1, S331.

Skedros, J.G., Bloebaum, R.D., Mason, M.W., Bramble, D.M., 1994. Analysis of a tension/compression skeletal system: possible strain-specific differences in the hierarchical organization of bone. Anat. Rec. 239, 396–404.

Skedros, J.G., Hughes, D.E., Nelson, K., Winet, H., 1999. Collagen fiber orientation in the proximal femur: challenging Wolff's tension/compression interpretation. J. Bone Miner Res. 14, S441.

Skedros, J.G., Brady, J., Sybrowsky, C.L., 2002. Mathematical analysis of trabecular trajectories in apparent trajectorial structures: the unfortunate historical emphasis on the human proximal femur. Am. J. Phys. Anthropol. 33, 142.

Skedros, J.G., Hunt, K.J., Bloebaum, R.D., 2004. Relationships of loading history and structural and material characteristics of bone: development of the mule deer calcaneus. J. Morphol. 259, 281–307.

Skerry, T., 2000. Biomechanical influences on skeletal growth and development. In: O'Higgins, P., Cohn, M.J. (Eds.), Development, Growth, and Evolution: Implications for the Study of the Homonid Skeleton. Academic Press, San Diego, CA, pp. 30–39.

Skerry, T.M., Lanyon, L.E., 1995. Interruption of disuse by short duration walking exercise does not prevent bone loss in the sheep calcaneus. Bone 16, 269–274.

Smith, J.W., 1962a. The relationship of epiphysial plates to stress in some bones of the lower limb. J. Anat. London 96, 58–78.

Smith, J.W., 1962b. The structure and stress relations of fibrous epiphysial plates. J. Anat. London 96, 209–225.

Solger, B., 1899. Der gegenwärtige stand der lehre von der knochen-aechitecur. Moleschott's Untersuchungen zur Naturlehre des Menschen und der Thiere XVI:, 187–219.

Stanford, C.M., Brand, R.A., 1999. Toward an understanding of implant occlusion and strain adaptive bone modeling and remodeling. J. Prosthet. Dent. 81, 553–561.

Stanford, C.M., Schneider, G.B., 2004. Functional behaviour of bone around dental implants. Gerodontology 21, 71–77.

Stauber, M., Rapillard, L., Van Lenthe, G.H., Zysset, P., Muller, R., 2006. Important of individual rods and plates in the assessment of bone quality and their contribution to bone stiffness. J. Bone Miner. Res. 21, 586–595.

Stephen, L., Lee, S., 1964. William Fairbairn. In: The Dictionary of National Biography. Oxford University Press, Oxford, UK, pp. 987–989.

Su, S.C., 1998. Microstructure and Mineral Content Correlations to Strain Parameters in Cortical Bone of the Artiodactyl Calcaneus. University of Utah, Salt Lake City, UT, p. 64.

Su, S.C., Skedros, J.G., Bachus, K.N., Bloebaum, R.D., 1999. Loading conditions and cortical bone construction of an artiodactyl calcaneus. J. Exp. Biol. 202, 3239–3254.

Swartz, S., Parker, A., Huo, C., 1998. Theoretical and empirical scaling patterns and topological homology in bone trabeculae. J. Exp. Biol. 201, 573–590.

Tachdjian, M.O., 1990. Developmental coxa vara. In: Pediatric orthopedics. WB Saunders Co, Philadelphia, PA, p. 585.
Tanck, E., Hannink, G., Ruimerman, R., Buma, P., Burger, E., Huiskes, R., 2006. Cortical development under the growth plate is regulated by mechanical load transfer. J. Anat. 208, 73–79.
Teng, S., Herring, S.W., 1995. A stereological study of trabecular architecture in the mandibular condyle of the pig. Arch. Oral. Biol. 40, 299–310.
Thompson, A., 1902. The relation of structure and function as illustrated by the form of the lower epiphysial suture of the femur. J. Anat. London 36, 95–105.
Thompson, D.W., 1917. On Growth and Form. Cambridge University Press, Cambridge, UK, p. 793.
Thompson, D.W., 1943. On form and mechanical efficiency. In: On Growth and Form. MacMillan Company, New York, pp. 958–1005.
Thomason, J.J., 1995. To what extent can the mechanical environment of a bone be inferred from its internal architecture? In: Thomason, J.J. (Ed.), Functional Vertebrate Morphology in Vertebrate Paleontology. Cambridge University Press, Cambridge, UK, pp. 249–277.
Thorpe, S.K., Crompton, R.H., Gunther, M.M., Ker, R.F., McNeill Alexander, R., 1999. Dimensions and moment arms of the hind- and forelimb muscles of common chimpanzees (Pan troglodytes). Am. J. Phys. Anthropol. 110, 179–199.
Tillman, B., Bartz, B., Schleider, A., 1985. Stress in the human ankle joint: a brief review. Arch. Orthop. Trauma Surg. 103, 385–391.
Tobin, W., 1955. The internal architecture of the femur and its clinical significance. J. Bone Joint Surg. 37-A, 57–71.
Tobin, W., 1968. An atlas of the comparative anatomy of the upper end of the femur. Clin. Orthop. Rel. Res. 56, 83–103.
Treharne, R.W., 1981. Review of Wolff's law and its proposed means of operation. Orthop. Rev. 10, 35–47.
Triepel, H., 1922. Die Architektur der knochenspongiosa in neuer Auffassung. Z. Knostitutionslehre 8, 269–311.
Trueta, J., 1968. Studies of the Development and Decay of the Human Frame. W.B. Saunders Co., Philadelphia, PA, p. 389.
Tsubota, K., Adachi, T., Tomita, Y., 2002. Functional adaptation of cancellous bone in human proximal femur predicted by trabecular surface remodeling simulation toward uniform stress state. J. Biomech. 35, 1541–1551.
Turner, C.H., 1992. On Wolff's law of trabecular architecture. J. Biomech. 25, 1–9.
Turner, C.H., Owan, I., Takano, Y., 1995. Mechanotransduction in bone: role of strain rate. Am. J. Physiol. 269, E438–E442.
Van Audekercke, R., Van der Perre, G., 1994. The effect of osteoporosis on the mechanical properties of bone structures. Clin Rheumatol. Suppl, 38–44.
Van Rietbergen, B., Huiskes, R., Eckstein, F., Ruegsegger, P., 2003. Trabecular bone tissue strains in the healthy and osteoporotic human femur. J. Bone Miner Res. 18, 1781–1788.
Vander Sloten, J., Van der Perre, G., 1989. Trabecular structure compared to stress trajectories in the proximal femur and the calcaneus. J. Biomed. Eng. 11, 203–208.
Venieratos, D., Papadopoulos, N.J., Anastassiou, J., Katritsis, E.D., 1987. A quantitative Estimation of the divergence between the trabecular system and the stress trajectories in the upper end of the human femoral bone. Anat. Anz. 163, 301–310.
Viola, T., 2002. Locomotion dependent variation in the proximal femoral trabecular pattern in primates. Institute of Anthropology, University of Vienna, Austria. Ph.D. Thesis, 123.
von Meyer, G.H., 1867. Die Architekur der Spongiosa. Arch. Anat. Physiol. Wissenschaf. Med. 34, 615–628.
Wang, X., Niebur, G.L., 2006. Microdamage propagation in trabecular bone due to changes in loading mode. J. Biomech. 39, 781–790.
Ward, S., Sussman, R., 1979. Correlates between locomotor anatomy and behavior in two sympatric species of Lemur. Am. J. Phys. Anthropol. 50, 575–590.
Whedon, G.D., Heaney, R.P., 1993. Effects of physical inactivity, paralysis, and weightlessness on bone growth. In: Hall, B.K. (Ed.), Bone: Bone Growth, vol. 7. CRC Press, Boca Raton, FL, pp. 57–78.
Williams, J.L., Do, P.D., Eick, J.D., Schmidt, T.L., 2001. Tensile properties of the physis vary with anatomic location, thickness, strain rate and age. J. Orthop. Res. 19, 1043–1048.
Williams, J.L., Vani, J.N., Eick, J.D., Petersen, E.C., Schmidt, T.L., 1999. Shear strength of the physis varies with anatomic location and is a function of modulus, inclination, and thickness. J. Orthop. Res. 17, 214–222.
Wolff, J., 1869. Uber die bedeutung der architektur der spongiösen substanz für die frage vom knochenwachsthum. Central. Med. Wissenschaf.: VII Jahrgang 54, 849–851.
Wolff, J., 1870. Uber die innere architektur der knochen und ihre bedeutung für die frage vom knochenwachstum. Arch. Pathol. Anat. Physiol. Klin. Med. 50, 389–453.
Wolff, J., 1872. Beiträge zur lehre von der heilung der fracturen. Arch. Klin. Chirurgie 14, 270–312.
Wolff, J., 1874. Zur Knochenwachsthumsfrage. Arch. Pathol. Anat. Physiol. Klin. Med. 61, 417–456.
Wolff, J., 1892. Das Gesetz der Transformation der Knochen. Springer, Berlin, Germany, p. 126.
Wolff, J., 1986. The Law of Bone Remodeling. Springer, Berlin, Germany, p. 126.
Woo, S.L., Kuei, S.C., Amiel, D., Gomez, M.A., Hayes, W.C., White, F.C., Akeson, W.H., 1981. The effect of prolonged physical training on the properties of long bone: a study of Wolff's Law. J. Bone Joint Surg. 63-A, 780–787.
Yamada, H., 1970. Strength of Biological Materials. Williams and Wilkins Co., Baltimore, MD, pp. 23–30.
Zippel, H., 1992. Julius Wolff and the law of bone remodeling. In: Regling, G. (Ed.), Wolff's Law and Connective Tissue Regulation. Walter de Gruyter, New York, pp. 1–12.
Zschokke, E., 1892. Weitere Untersuchungen uber das Verhaltniss der Knochenbildung zur Statik und Mechanik des Vertebraten-Skelettes. Zurich, Switzerland, p. 102.
Zylstra, M., 2000. Trabecular architecture of metacarpal heads in catarrhines: a preliminary report. Am. J. Phys. Anthropol. 30, 331.